

Fermion masses and mixings and charged lepton flavor violation in a 3-3-1 model with inverse seesaw

A. E. Cárcamo Hernández,^{1,2,3,*} D. T. Huong,^{4,†} H. N. Long,^{5,6,‡} and Daniel Salinas-Arizmendi^{1,2,§}

¹*Departamento de Física, Universidad Técnica Federico Santa María Casilla 110-V, Valparaíso, Chile*

²*Centro Científico-Tecnológico de Valparaíso, Casilla 110-V, Valparaíso, Chile*

³*Millennium Institute for Subatomic Physics at the High-Energy Frontier, SAPHIR, Calle Fernández Concha No 700, Santiago, Chile*

⁴*Institute of Physics, Vietnam Academy of Science and Technology, 10 Dao Tan, Ba Dinh, Hanoi, Vietnam*

⁵*Subatomic Physics Research Group, Science and Technology Advanced Institute, Van Lang University, Ho Chi Minh City 70000, Vietnam*

⁶*Faculty of Applied Technology, School of Technology, Van Lang University, Ho Chi Minh City 70000, Vietnam*

(Dated: June 18, 2025)

We present an extension of the 3-3-1 gauge model supplemented by an A_4 flavor symmetry and cyclic discrete symmetries, including Z_2 , Z'_2 , Z_3 , Z_4 , Z_7 and Z_{10} . The model successfully reproduces the observed SM fermion mass hierarchies and mixing patterns in quark and lepton sectors. The smallness of the active neutrino masses is explained through an inverse seesaw mechanism, enabled by the introduction of right-handed and sterile Majorana neutrinos. In the quark sector, flavor-changing neutral currents (FCNCs) arise at tree level exclusively for up-type quarks via the new heavy neutral gauge boson exchange, leading to strong constraints from $D^0-\bar{D}^0$ mixing. The charged lepton sector exhibits sizeable flavor-violating effects, especially in the $\mu \rightarrow e\gamma$ decay, mediated by loops involving heavy neutrinos, new charged gauge bosons as well as charged scalars. We perform a detailed numerical fit of fermion masses and mixing parameters and identify viable regions of parameter space consistent with experimental data on CKM and PMNS mixing matrices. The model predicts branching ratios for charged lepton flavor violating decays and $\mu-e$ conversion rates within the sensitivity of future experiments.

I. INTRODUCTION

Despite the remarkable consistency of the Standard Model (SM) predictions with the experimental data, several issues remain unresolved. One such issue is the nonzero neutrino masses, confirmed by various neutrino oscillation experiments [1–3]. Additionally, the SM fails to account for the observed dark matter relic abundance and the matter-antimatter asymmetry of the Universe [4]. Furthermore, the SM cannot explain the existence of three fermion generations, the quantization of the electric charge, and the hierarchical structure of charged fermion masses. These shortcomings necessitate a more comprehensive theory, of which the SM may be considered a low energy effective theory. The SM also fails to explain the significant disparity between quark and lepton mixing patterns. While the Cabibbo-Kobayashi-Maskawa (CKM) matrix [5, 6] quantifies the misalignment between up- and down-quark Yukawa couplings, exhibiting a hierarchical structure with dominant diagonal elements, the Pontecorvo-Maki-Nakagawa-Sakata (PMNS) matrix [7] deviates significantly from diagonality. The discovery of neutrino oscillations has established the existence of lepton flavor violation. However, the SM predicts negligible rates for such processes [8–11], like $\mu \rightarrow e\gamma$. To address this discrepancy and other shortcomings, various theories beyond the Standard Model (BSM) have been proposed. These BSM models, such as low-scale seesaw models, often predict enhanced rates for LFV decays, bringing them within the reach of current and future experiments.

The assumption of underlying BSM physics to explain the SM fermion mass hierarchies and mixing patterns [12–55] may provide valuable clues to the nature of new physics (NP). The extension of the SM gauge symmetry to a higher weak isospin symmetry $SU(3)_L$, is a well-known framework for addressing the number of fermion generations, commonly referred to as the 3-3-1 model when including color and electric charges [56–59]. In addition to explaining the number of fermion families, this new gauge principle offers potential solutions to fundamental questions such as

* antonio.carcamo@usm.cl

† dthuong@iop.vast.ac.vn

‡ hoangngoclong@vlu.edu.vn

§ daniel.salinas@usm.cl

electric charge quantization [60–63], the strong CP conservation [64–66]. Furthermore, it naturally addresses issues related to neutrino mass generation [67–82], flavor physics [83–94], dark matter stability [95–113], and even cosmic inflation and baryon asymmetry [114–116].

The A_4 discrete flavour group has been used widely in the literature, due to its high predictive power and since it provides a nice description of the SM fermion mass and mixing pattern [12–55, 117, 118]. We adopt the A_4 group as discrete flavor symmetry of the $SU(3)_C \times SU(3)_L \times U(1)_X$ 3-3-1 model, leveraging its unique three-dimensional irreducible representation to naturally accommodate the three fermion families. The spontaneous breaking of symmetries generates the SM fermion mass and mixing patterns. The absence of exotic electric charges in fermion sector allows for low-scale linear or inverse seesaw mechanism, generating tiny neutrino masses and potentially testable sterile neutrino at the $SU(3)_L \times U(1)_X$ breaking scale. Our model employs the inverse seesaw mechanism to generate light neutrino masses, thus making the model testable at the colliders.

The remainder of the paper is organized as follows. In Section II, we present the proposed model. Section III analyzes the implications of the model for quark masses and mixings. Lepton masses and mixings are discussed in Section IV. The scalar and gauge sectors of the model are detailed in Section V. Section VI contains an analysis and discussion of the flavor-changing neutral currents. Section VII derives the constraints on the model parameter space imposed by charged lepton flavor violating decays. We conclude in section VIII.

II. THE MODEL

We propose an extension of the economical 3-3-1 model with three right handed Majorana neutrinos, where the $SU(3)_C \times SU(3)_L \times U(1)_X$ gauge symmetry is supplemented by the $U(1)_{L_g}$ global lepton number symmetry and the $A_4 \times Z_2 \times Z'_2 \times Z_3 \times Z_4 \times Z_7 \times Z_{10}$ discrete group. In this model, the scalar sector consists of two $SU(3)_L$ scalar triplets and several gauge singlet scalars, introduced to generate viable and predictive SM fermion mass matrices that are consistent with the low energy SM fermion flavor data. The scalar and fermionic spectra, along with their transformations under the $SU(3)_C \times SU(3)_L \times U(1)_X \times U(1)_{L_g} \times A_4 \times Z_2 \times Z'_2 \times Z_3 \times Z_4 \times Z_7 \times Z_{10}$ group, are presented in Tables I and II, respectively. The dimensions of the $SU(3)_C$, $SU(3)_L$ and A_4 representations shown in Tables I and II are indicated by boldface numbers, while the different $U(1)_X$ and Z_N charges are written in additive notation. Note that a field ψ transforms under the Z_N symmetry with a corresponding q_n charge as: $\psi \rightarrow e^{\frac{2\pi i q_n}{N}} \psi$, $n = 0, 1, 2, 3 \dots N - 1$. We choose the A_4 symmetry because it is the smallest nonabelian group possessing triplet and three singlet irreducible representations (as detailed in Appendix A), thus allowing us to naturally accommodate the three families of SM fermions. Additionally, the A_4 , Z_3 , Z_4 and Z_7 symmetries select the allowed entries of the SM down-type quark mass matrices and determine the hierarchical pattern among these entries, which is necessary to correctly reproduce the observed SM fermion mass and mixing structure. In addition to that, the Z_2 and Z_3 symmetries naturally explain the small values of the electron and down quark masses. The Z_{10} symmetry separates the A_4 scalar triplets participating in the quark and neutrino Yukawa interactions from the ones appearing in the charged lepton Yukawa terms, thus allowing one to treat these sectors independently. Finally, the Z'_2 symmetry is crucial for obtaining a nearly diagonal sterile neutrino mass matrix with non-degenerate sterile neutrinos. In our model, the masses for the SM charged fermions lighter than the top quark arise from non-renormalizable Yukawa interactions, after the spontaneous breaking of the discrete symmetries. Consequently, the spontaneous breaking of the $A_4 \times Z_2 \times Z'_2 \times Z_3 \times Z_4 \times Z_7 \times Z_{10}$ discrete group generates the observed pattern of SM fermion masses and mixing angles. The light active neutrino masses are generated through an inverse seesaw mechanism, where the smallness of its μ parameter is naturally explained by having higher dimensional Yukawa interactions involving gauge singlet scalar fields charged under the model's various discrete symmetries. Upon spontaneous breaking of these discrete symmetries, small lepton number violating Majorana mass terms are generated, leading to the μ parameter in the inverse seesaw mechanism. It is worth mentioning that the $U(1)_{L_g}$ global lepton number symmetry is spontaneously broken down to a residual discrete $Z_2^{(L_g)}$ by the vacuum expectation values (VEVs) of the $U(1)_{L_g}$ charged gauge-singlet scalars ξ_i ($i = 1, 2, 3$), φ having a nontrivial $U(1)_{L_g}$ charge, as indicated by Table I. The residual discrete $Z_2^{(L_g)}$ lepton number symmetry, under which the leptons are charged and the other particles are neutral, prevents the appearance of interactions involving an odd number of leptons, which is crucial to guarantee the stability of the proton. The corresponding massless Goldstone boson arising from the spontaneous breaking of the $U(1)_{L_g}$ global symmetry, i.e., the Majoron, is a $SU(3)_L$ scalar singlet, which does not cause any problems in our model. Additionally, the fermions in our model do not exhibit exotic electric charges. Consequently, the electric charge assumes the following form

$$Q = T_3 + \beta T_8 + XI = T_3 - \frac{1}{\sqrt{3}} T_8 + XI, \quad (1)$$

with $I = \text{diag}(1, 1, 1)$, $T_3 = \frac{1}{2}\text{diag}(1, -1, 0)$ and $T_8 = \left(\frac{1}{2\sqrt{3}}\right)\text{diag}(1, 1, -2)$ for a $SU(3)_L$ triplet. The X parameter represents the charge associated with the $U(1)_X$ gauge group. The lepton number is defined as [69, 119–121]:

$$L = \frac{4}{\sqrt{3}}T_8 + L_g, \quad (2)$$

where L_g is a conserved charge associated with the $U(1)_{L_g}$ global lepton number symmetry. The full symmetry \mathcal{G} features the following symmetry breaking pattern:

$$\begin{aligned} \mathcal{G} &= SU(3)_C \times SU(3)_L \times U(1)_X \times U(1)_{L_g} \times A_4 \times Z_2 \times Z'_2 \times Z_3 \times Z_4 \times Z_7 \times Z_{10} \xrightarrow{\Lambda_{\text{int}}} \\ &SU(3)_C \times SU(3)_L \times U(1)_X \times U(1)_{L_g} \xrightarrow{v_\chi} SU(3)_C \times SU(2)_L \times U(1)_Y \times U(1)_{L_g} \\ &\xrightarrow{v_\rho, v_\varphi, v_\xi} SU(3)_C \times U(1)_Q \times Z_2^{(L_g)}. \end{aligned} \quad (3)$$

To be consistent with the SM result, the symmetry breaking scales must satisfy the following hierarchy: $\Lambda_{\text{int}} > v_\chi \gg v_\rho, v_\varphi, v_\xi$. The $SU(3)_L$ triplet scalar fields χ and ρ are represented as:

$$\chi = \begin{pmatrix} \frac{1}{\sqrt{2}}(\xi'_\chi \pm i\zeta'_\chi) \\ \chi_2^- \\ \frac{1}{\sqrt{2}}(v_\chi + \xi_\chi \pm i\zeta_\chi) \end{pmatrix}, \quad \rho = \begin{pmatrix} \rho_1^+ \\ \frac{1}{\sqrt{2}}(v_\rho + \xi_\rho \pm i\zeta_\rho) \\ \rho_3^+ \end{pmatrix} \quad (4)$$

The $SU(3)_L$ fermionic triplets and antitriplets are given by:

$$Q_{1L} = \begin{pmatrix} u_1 \\ d_1 \\ J_1 \end{pmatrix}_L, \quad Q_{nL} = \begin{pmatrix} d_n \\ -u_n \\ J_n \end{pmatrix}_L, \quad L_{iL} = \begin{pmatrix} \nu_{iL} \\ l_{iL} \\ \nu_{iR}^c \end{pmatrix}, \quad n = 2, 3, \quad i = 1, 2, 3. \quad (5)$$

With the particle spectrum and symmetries specified in Tables I and II, we have the following relevant Yukawa terms

	χ	ρ	σ_1	σ_2	σ_3	η	ζ	ϑ	ϕ	Φ	Ξ	ξ	φ	S_1	S_2
$SU(3)_C$	1	1	1	1	1	1	1	1	1	1	1	1	1	1	1
$SU(3)_L$	3	3	1	1	1	1	1	1	1	1	1	1	1	1	1
$U(1)_X$	$-\frac{1}{3}$	$\frac{2}{3}$	0	0	0	0	0	0	0	0	0	0	0	0	0
$U(1)_{L_g}$	$\frac{4}{3}$	$-\frac{2}{3}$	0	0	0	0	0	0	0	0	0	2	2	0	0
A_4	1	1	1'	1'	1''	3	3	3	3	3	3	3	1'	1'	1''
Z_2	1	0	0	0	1	0	0	0	0	0	0	1	1	0	0
Z'_2	0	0	0	0	0	0	0	0	0	0	0	0	0	1	1
Z_3	0	0	1	1	0	0	0	0	0	0	0	0	0	0	0
Z_4	0	0	-1	0	0	0	0	0	0	0	0	2	2	0	0
Z_7	0	0	0	-1	-3	0	0	0	0	0	0	0	0	0	0
Z_{10}	0	0	0	0	0	0	-5	-5	-3	-1	-1	0	0	0	0

Table I: Scalar assignments under $SU(3)_C \times SU(3)_L \times U(1)_X \times U(1)_{L_g} \times A_4 \times Z_2 \times Z'_2 \times Z_3 \times Z_4 \times Z_7 \times Z_{10}$.

for both quark and lepton sectors:

$$\begin{aligned} -\mathcal{L}_Y^{(q)} &= y_1^{(J)} \bar{Q}_{1L} \chi J_{1R} + \sum_{n=2}^3 y_n^{(J)} \bar{Q}_{nL} \chi^* J_{nR} + y_{33}^{(u)} \bar{Q}_{3L} \rho^* u_{3R} + y_{23}^{(u)} \bar{Q}_{2L} \rho^* u_{3R} \frac{\sigma_1^2}{\Lambda^2} \\ &+ y_{13}^{(u)} \varepsilon_{abc} \bar{Q}_{1L}^a (\rho^*)^b (\chi^*)^c u_{3R} \frac{(\sigma_1^*)^2}{\Lambda^3} + y_{12}^{(u)} \varepsilon_{abc} \bar{Q}_{1L}^a (\rho^*)^b (\chi^*)^c u_{2R} \frac{(\sigma_2^*)^3}{\Lambda^4} + y_{22}^{(u)} \bar{Q}_{2L} \rho^* u_{2R} \frac{\sigma_2^4}{\Lambda^4} \\ &+ y_{11}^{(u)} \varepsilon_{abc} \bar{Q}_{1L}^a (\rho^*)^b (\chi^*)^c u_{1R} \frac{\sigma_2^4 \sigma_1^2}{\Lambda^7} + \frac{1}{\Lambda^2} y_3^{(d)} \varepsilon_{abc} \bar{Q}_{3L} \rho^b \chi^c (\eta D_R)_1 \\ &+ y_2^{(d)} \varepsilon_{abc} \bar{Q}_{2L} \rho^b \chi^c (\eta D_R)_{1''} \frac{\sigma_1^2}{\Lambda^4} + y_1^{(d)} \bar{Q}_{1L} \rho (\eta D_R)_{1'} \frac{(\sigma_1^*)^2 (\sigma_2^*)^3 \sigma_3}{\Lambda^7} + H.c., \end{aligned} \quad (6)$$

	Q_{1L}	Q_{2L}	Q_{3L}	u_{1R}	u_{2R}	u_{3R}	D_R	J_{1R}	J_{2R}	J_{3R}	L_L	l_{1R}	l_{2R}	l_{3R}	N_R
$SU(3)_C$	3	3	3	3	3	3	3	3	3	3	1	1	1	1	1
$SU(3)_L$	3	$\bar{\mathbf{3}}$	$\bar{\mathbf{3}}$	1	1	1	1	1	1	1	3	1	1	1	1
$U(1)_X$	$\frac{1}{3}$	0	0	$\frac{2}{3}$	$\frac{2}{3}$	$\frac{2}{3}$	$-\frac{1}{3}$	$\frac{2}{3}$	$-\frac{1}{3}$	$-\frac{1}{3}$	$-\frac{1}{3}$	-1	-1	-1	0
$U(1)_{L_q}$	$-\frac{2}{3}$	$\frac{2}{3}$	$\frac{2}{3}$	0	0	0	0	-2	2	2	$\frac{1}{3}$	1	1	1	-1
A_4	1'	1''	1	1'	1'	1	3	1'	1''	1	3	1'	1''	1'	3
Z_2	1	1	1	0	0	1	0	0	0	0	0	1	0	0	0
Z'_2	0	0	0	0	0	0	0	0	0	0	0	0	0	0	1
Z_3	1	-1	0	1	1	0	0	1	-1	0	0	0	-1	1	0
Z_4	0	0	2	2	0	2	2	0	0	2	1	-1	1	-1	1
Z_7	0	0	0	4	4	0	0	0	0	0	0	0	-3	0	0
Z_{10}	0	0	0	0	0	0	0	0	0	0	0	5	3	1	0

Table II: Fermion assignments under $SU(3)_C \times SU(3)_L \times U(1)_X \times U(1)_{L_q} \times A_4 \times Z_2 \times Z'_2 \times Z_3 \times Z_4 \times Z_7 \times Z_{10}$.

$$\begin{aligned}
-\mathcal{L}_Y^{(l)} = & y_1^{(l)} (\bar{L}_L \rho \zeta)_{\mathbf{1}} l_{1R} \frac{\sigma_2^4 \sigma_1^2 \sigma_3}{\Lambda^8} + y_2^{(l)} (\bar{L}_L \rho \phi)_{\mathbf{1}} l_{2R} \frac{\sigma_2^4}{\Lambda^5} + y_3^{(l)} (\bar{L}_L \rho \Phi)_{\mathbf{1}} l_{3R} \frac{\sigma_1^2}{\Lambda^3} \\
& + z_1^{(l)} (\bar{L}_L \rho \vartheta)_{\mathbf{1}} l_{1R} \frac{\sigma_2^4 \sigma_1^2 \sigma_3}{\Lambda^8} + z_3^{(l)} \bar{L}_L (\rho \Xi)_{\mathbf{1}} l_{3R} \frac{\sigma_1^2}{\Lambda^3} \\
& + y_{1\chi}^{(L)} (\bar{L}_L \chi N_R)_{\mathbf{1}'} \frac{S_1}{\Lambda} + y_{2\chi}^{(L)} (\bar{L}_L \chi N_R)_{\mathbf{1}'} \frac{S_2}{\Lambda} + x_\rho \varepsilon_{abc} (\bar{L}_L^a (L_L^C)^b)_{\mathbf{3a}} (\rho^*)^c \frac{\eta \sigma_1^2}{\Lambda^3} \\
& + y_{1N} (N_R \overline{N_R^C})_{\mathbf{3s}} \xi \frac{\sigma_2^4 \sigma_1^2 \sigma_3}{\Lambda^7} + y_{2N} (N_R \overline{N_R^C})_{\mathbf{1}} \varphi \frac{\sigma_2^4 \sigma_1^2 \sigma_3}{\Lambda^7} + H.c.,
\end{aligned} \tag{7}$$

where the subscripts **1**, **1'**, **1''**, **3s**, **3a** denote the irreducible representations under the discrete symmetry group A_4 . The corresponding tensor products are detailed in Appendix A.

In our model, the Yukawa terms contain several non-renormalizable interactions, as observed in Eqs. (6) and (7). These operators arise at high energies, where heavy mediators induce effective terms at low energies. They allow for an explanation of the fermion mass hierarchy without fine-tuning. Additionally, these operators may play a key role in generating light neutrino masses within the inverse seesaw mechanism. These operators have a general structure of the form

$$\overline{\psi}_L H_1 H_2 \Psi_R \frac{H_3^n}{\Lambda^{n+1}}, \tag{8}$$

where ψ_L and Ψ_L are fermions, H_i are scalar fields that acquire VEVs, generating the observed hierarchy in the fermion masses. The non-renormalizable operators could arise from a more fundamental theory with new scalar fields and heavy fermions. In particular, the effective operators in (6) and (7) may originate from the following renormalizable interactions

$$\overline{\psi}_L H_4 \tilde{\Psi}_R, \tag{9}$$

where the fermions $\tilde{\Psi}$ is heavy intermediate states that, once integrated out of the low-energy spectrum, induce the effective operators appearing in our model. The Yukawa operators of non-normalizable up and down quarks are has a possible ultraviolet origin of the non-renormalizable terms is that they are generated at low energies through the Feynman diagrams presented in Figure 1, where H'_i are mediator fields with masses on the order of the model cutoff scale Λ_{int} . Meanwhile, the non-renormalizable lepton Yukawa operators can be generated at low energies from the Feynman diagrams shown in Figure 2.

In order to comply with the current data on SM fermion masses and mixing angles with less parameters than observables (especially in the lepton sector), we consider the following VEV patterns for the A_4 triplets gauge singlet

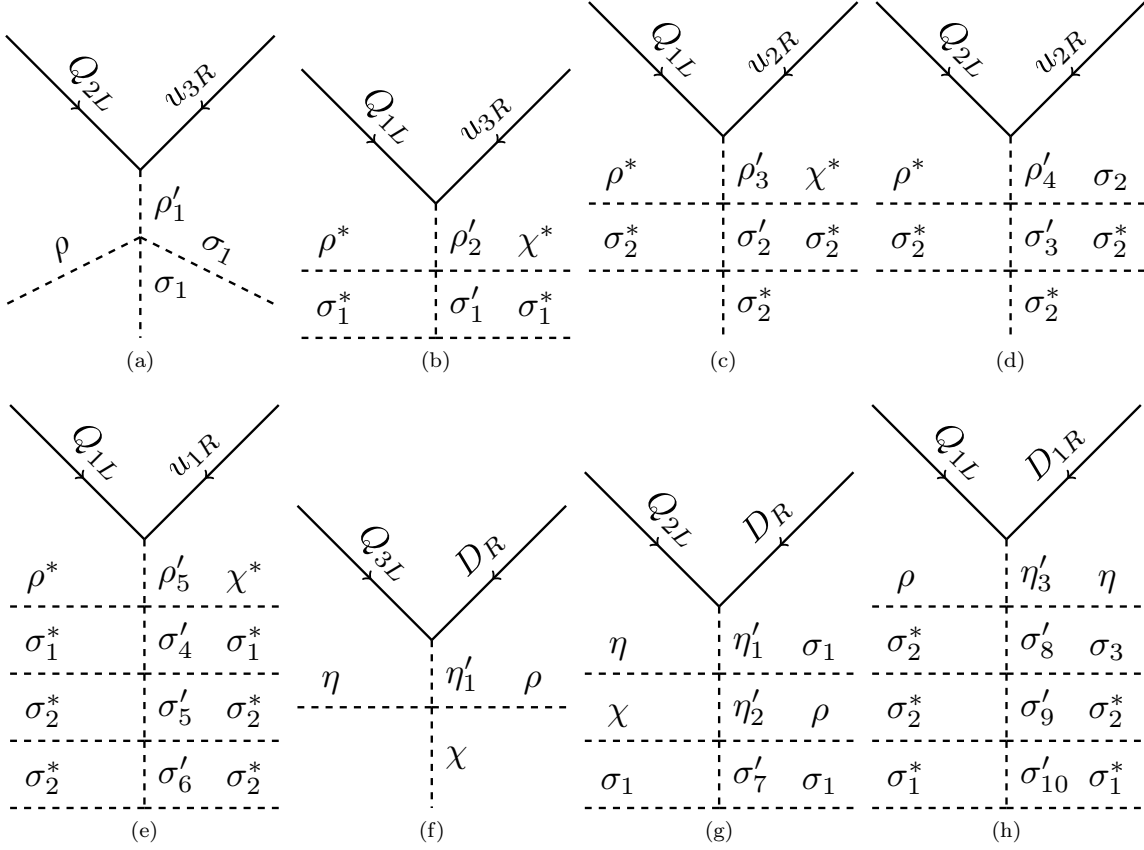


Figure 1: Feynman diagrams that induce the non-renormalizable operators in quark sector.

scalars:

$$\langle \eta \rangle = \frac{v_\eta}{\sqrt{3}} (1, 1, 1), \quad \langle \xi \rangle = \frac{v_\xi}{\sqrt{3}} (1, -1, 1), \quad (10)$$

$$\langle \zeta \rangle = \frac{v_\zeta \cos \alpha}{\sqrt{3}} (\cos \alpha - \sin \alpha, \cos \alpha - \omega \sin \alpha, \cos \alpha - \omega^2 \sin \alpha), \quad \langle \vartheta \rangle = \frac{v_\vartheta \omega^2 \sin \alpha}{\sqrt{3}} (1, \omega^2, \omega), \quad (11)$$

$$\langle \phi \rangle = \frac{v_\phi}{\sqrt{3}} (\cos \alpha + \sin \alpha, \omega \cos \alpha + \sin \alpha, \omega^2 \cos \alpha + \sin \alpha), \quad (12)$$

$$\langle \Phi \rangle = -\frac{v_\Phi \omega \sin \alpha}{\sqrt{3}} (\cos \alpha - \sin \alpha, \cos \alpha - \omega \sin \alpha, \cos \alpha - \omega^2 \sin \alpha) \quad (13)$$

$$\langle \Xi \rangle = \frac{v_\Xi \cos \alpha}{\sqrt{3}} (1, \omega^2, \omega), \quad \omega = e^{\frac{2\pi i}{3}}, \quad (14)$$

which are consistent with the scalar potential minimization equations for a large region of parameter space.

Given that the breaking of the $A_4 \times Z_2 \times Z_3 \times Z_4 \times Z_7 \times Z_{10}$ discrete group produces the SM charged fermion mass and quark mixing pattern, we set the VEVs of the $SU(3)_L$ singlet scalar fields with respect to the Wolfenstein parameter $\lambda = 0.225$ and the model cutoff Λ . If the gauge symmetry break as patterns given in (3), we have

$$v_\rho \sim v_\xi \sim v_\varphi \sim \lambda^5 \Lambda \ll v_\chi \sim \lambda^2 \Lambda < v_{\sigma_i} \sim v_{S_k} \sim v_\eta \sim v_\zeta \sim v_\vartheta \sim v_\phi \sim v_\Phi \sim v_\Xi \sim \lambda \Lambda, \quad i = 1, 2, 3, \quad k = 1, 2, \quad (15)$$

where the model cutoff Λ is the scale of the UV completion of the model, which can corresponds to the mass scale of the Froggatt-Nielsen messenger fields.

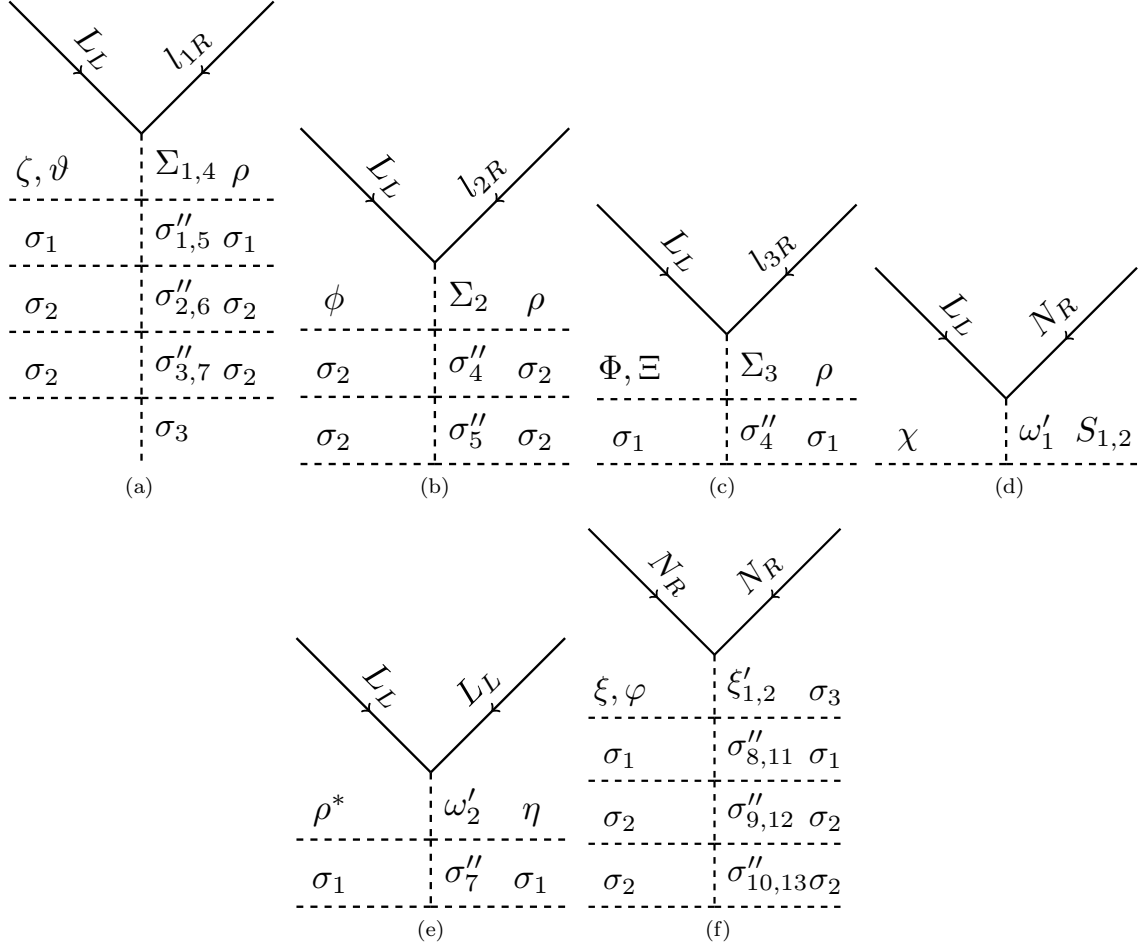


Figure 2: Feynman diagrams that induce the non-renormalizable operators in lepton sector.

III. QUARK MASSES AND MIXINGS

The quark Yukawa terms of Eq. (6) give rise to the following SM mass matrices for quarks:

$$\begin{aligned}
 M_U &= \frac{v_\rho}{\sqrt{2}} \begin{pmatrix} c_1 \lambda^8 & b_1 \lambda^5 & a_1 \lambda^4 \\ 0 & b_2 \lambda^4 & a_2 \lambda^2 \\ 0 & 0 & a_3 \end{pmatrix}, & M_D &= \frac{v_\rho}{\sqrt{2}} \begin{pmatrix} g_1 \lambda^7 & 0 & 0 \\ 0 & g_2 \lambda^5 & 0 \\ 0 & 0 & g_3 \lambda^3 \end{pmatrix} R_D, \\
 R_D &= \frac{1}{\sqrt{3}} \begin{pmatrix} 1 & 1 & 1 \\ 1 & \omega^2 & \omega \\ 1 & \omega & \omega^2 \end{pmatrix}, & & & (16)
 \end{aligned}$$

where c_1, b_n ($n = 1, 2$), a_i, g_i ($i = 1, 2, 3$) are $\mathcal{O}(1)$ dimensionless parameters, assumed to be real, excepting a_1 , which is taken to be complex. Notice that we take a_1 to be complex since the CP violating phase in the quark sector is associated with the quark mixing angle in the 1-3 plane, as indicated by the Standard parametrization of the CKM quark mixing matrix. In addition, notice that parameter $v_\rho = 246$ GeV corresponds to the scale of electroweak symmetry breaking. The SM quark mass matrices of Eq. (16), imply that the quark mixing angles are generated from the up type quark sector.

Furthermore, we find that the exotic quark masses are given by:

$$m_{J_i} = y_i^{(J)} \frac{v_\chi}{\sqrt{2}}, \quad i = 1, 2, 3. \quad (17)$$

The experimental values of the quark masses [122, 123], mixing angles and Jarlskog invariant [124] are well reproduced,

Observable	Model value	Experimental value
$m_u(\text{MeV})$	2.33 ± 0.15	$2.16^{+0.49}_{-0.26}$
$m_c(\text{GeV})$	1.26 ± 0.06	1.27 ± 0.02
$m_t(\text{GeV})$	172.52 ± 4.59	172.69 ± 0.30
$m_d(\text{MeV})$	4.52 ± 0.21	$4.67^{+0.48}_{-0.17}$
$m_s(\text{MeV})$	95.5 ± 5.6	$93.4^{+8.6}_{-3.4}$
$m_b(\text{GeV})$	4.19 ± 0.15	$4.18^{+0.03}_{-0.02}$
$\sin \theta_{12}^{(q)}$	0.225 ± 0.005	0.22500 ± 0.00067
$\sin \theta_{23}^{(q)}$	0.0419 ± 0.0024	$0.04182^{+0.00085}_{-0.00074}$
$\sin \theta_{13}^{(q)}$	0.00372 ± 0.00034	0.00369 ± 0.00011
J_q	$(3.35 \pm 0.43) \times 10^{-5}$	$(3.08^{+0.15}_{-0.13}) \times 10^{-5}$

Table III: Model and experimental values of the quark masses and CKM parameters.

as indicated in Table III. Consequently, the fit for the quark sector was performed by minimizing a χ_q^2 function, defined as,

$$\chi_q^2 = \sum_i \left(\frac{O_i^{\text{model}} - O_i^{\text{exp}}}{\sigma_i^{\text{exp}}} \right)^2 \quad (18)$$

where $O_i = \{m_i, \sin \theta_{ij}^{(q)}, J_q\}$, where m_i are the masses of the quarks ($i = u, c, t, d, s, b$), $\sin \theta_{ij}^{(q)}$ is the sine function of the quark mixing angles (with $j, k = 1, 2, 3$) and J_q is the quark Jarlskog invariant. The supra indices represent the experimental (exp) and theoretical (model) values, and the σ are the experimental errors. Obtaining the following values for our best-fit point for the following values of the quark sector parameters:

$$\begin{aligned} c_1 &\simeq -2.09 \pm 0.13, & b_1 &\simeq 2.84 \pm 0.14, & b_2 &\simeq 2.77 \pm 0.13, & |a_1| &\simeq 3.63 \pm 0.18, & a_2 &\simeq 0.80 \pm 0.03, \\ a_3 &\simeq 0.99 \pm 0.03, & g_1 &\simeq -0.89 \pm 0.04, & g_2 &\simeq 0.95 \pm 0.06, & g_3 &\simeq -2.12 \pm 0.07, & \arg(a_1) &\simeq 23.35 \pm 1.57^\circ. \end{aligned} \quad (19)$$

As shown in Table III, our model successfully fit for the ten physical observables in the quark sector. The symmetries inherent in our model enable us to successfully explain the SM quark mass spectrum and mixing parameters, with quark sector effective free parameters of order unity. The correlation between the quark mixing angle $\sin \theta_{13}$ and the Jarlskog invariant is depicted in Figure 3. In the left panel (a), we observe a heat-map for our model, revealing a strong correlation intensity in the $\sin \theta_{13}$ - J_q plane, with a correlation of 0.92. This indicates that the Jarlskog invariant is highly sensitive to variation in θ_{13} , aligning with the experimental observation of its small value. Conversely, variations in θ_{12} have a negligible impact on the Jarlskog invariant. A significant correlation is also observed in the $\sin \theta_{23}$ - J_q plane. By analyzing this heat map, we can refine our parameter space scan for our model of interest. As previously noted, the right panel (b) graphically illustrates the correlation between $\sin \theta_{13}$ and the Jarlskog invariant J_q . In this figure, the color represents the correlation in the $\sin \theta_{13}$ - $\sin \theta_{23}$ plane.

Finally, to close this section, we concisely discuss the collider signatures of the exotic quarks in our model. The exotic up type J_1 and down J_n ($n = 2, 3$) quarks can be produced in pairs via the gluon fusion mechanism and Drell-Yan annihilation. Once produced, they can decay in several ways: $J_1 \rightarrow H^+ d_i$, $J_1 \rightarrow W'^+ d_i$, while for the J_n quarks, the decay modes include $J_n \rightarrow H^- u_i$, $J_n \rightarrow W'^- u_i$ ($i = 1, 2, 3$). Here, H^\pm are physical electrically charged scalars associated with the third component of the $SU(3)_L$ ρ scalar triplet. The electrically charged scalars H^- (H^+) can further decay into the SM-charged lepton (antilepton) and neutrino. Consequently, the pair production of exotic quarks at a proton-proton collider can produce a final state composed of two jets, opposite sign dileptons, and missing energy. Thus, observing an excess of events involving the SM background in the opposite sign dileptons, two jets, and missing energy can be a possible signal of support of this model at the LHC. A detailed analysis of the collider signatures of exotic quarks in theories with extended $SU(3)_C \times SU(3)_L \times U(1)_X$ is provided in [125]. A comprehensive study of the exotic quark production and decay modes at colliders in our model goes beyond the scope of this work and is deferred for a future publication.

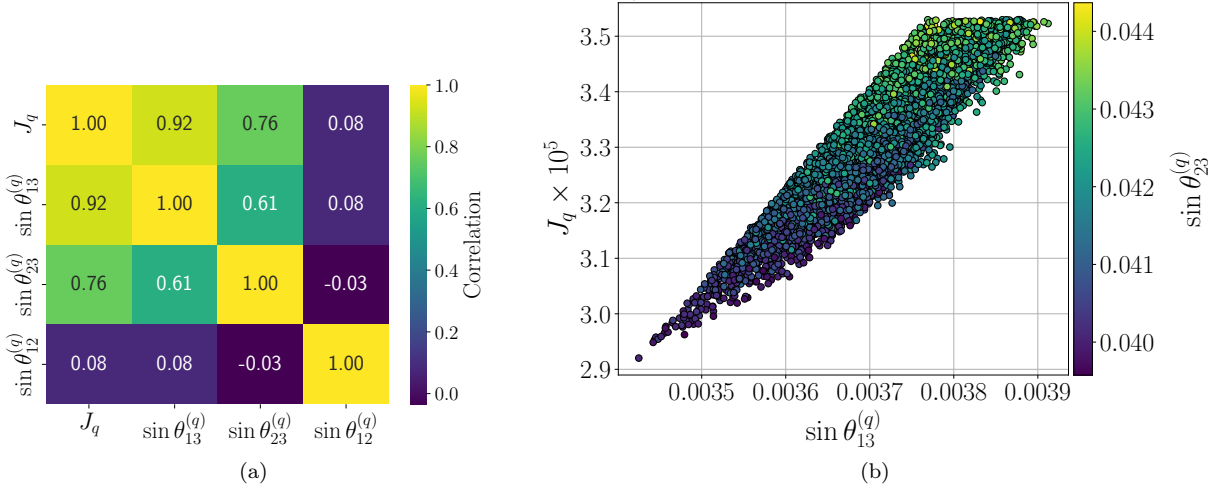


Figure 3: (a) Correlation heat-map: The correlation matrix between the quark mixing angle and the Jarlskog invariant J_q . (b) Correlation plot: A color plot depicting the correlation between $\sin \theta_{13}$ and J_q , where the color intensity signifies the correlation strength in the $\sin \theta_{13} - \sin \theta_{23}$ plane.

IV. LEPTON MASSES AND MIXINGS

The charged lepton Yukawa interactions yield the following mass matrix for charged leptons:

$$M_\ell = R_{\ell L} \text{diag}(m_e, m_\mu, m_\tau), \quad (20)$$

$$R_{\ell L} = \frac{1}{\sqrt{3}} \begin{pmatrix} 1 & 1 & 1 \\ 1 & \omega & \omega^2 \\ 1 & \omega^2 & \omega \end{pmatrix} \begin{pmatrix} \cos \alpha & \sin \alpha & 0 \\ -\sin \alpha & \cos \alpha & 0 \\ 0 & 0 & 1 \end{pmatrix} \begin{pmatrix} \cos \gamma & 0 & -\omega \sin \gamma \\ 0 & 1 & 0 \\ \omega^2 \sin \gamma & 0 & \cos \gamma \end{pmatrix},$$

where the charged lepton masses are:

$$m_e = a_1^{(\ell)} \lambda^8 \frac{v_\rho}{\sqrt{2}}, \quad m_\mu = a_2^{(\ell)} \lambda^5 \frac{v_\rho}{\sqrt{2}}, \quad m_\tau = a_3^{(\ell)} \lambda^3 \frac{v_\rho}{\sqrt{2}}. \quad (21)$$

where $a_i^{(\ell)} = y_i^{(\ell)}$ ($i = 1, 2, 3$) are $\mathcal{O}(1)$ parameters and we assumed that $y_{1,3}^{(\ell)} = z_{1,3}^{(\ell)}$. The neutrino Yukawa interactions of Eq. (7) yield the following neutrino mass terms:

$$-\mathcal{L}_{mass}^{(\nu)} = \frac{1}{2} \left(\overline{(\nu_L)^C} \quad \overline{\nu_R} \quad \overline{N_R} \right) M_\nu \begin{pmatrix} \nu_L \\ (\nu_R)^C \\ (N_R)^C \end{pmatrix} + H.c., \quad (22)$$

where $\nu_{iR} \equiv (\nu_{iL}^c)^C$, and the neutrino mass matrix reads:

$$M_\nu = \begin{pmatrix} 0_{3 \times 3} & M_{\nu D} & 0_{3 \times 3} \\ M_{\nu D}^T & 0_{3 \times 3} & M_\chi \\ 0_{3 \times 3} & M_\chi^T & M_R \end{pmatrix}, \quad (23)$$

and the sub matrices are given by:

$$\begin{aligned}
M_{\nu D} &= x_\rho \frac{v_\rho v_\eta v_{\sigma_1}^2}{2\Lambda^3} \begin{pmatrix} 0 & 1 & -1 \\ -1 & 0 & 1 \\ 1 & -1 & 0 \end{pmatrix}, \\
M_\chi &= y_{1\chi}^{(L)} \frac{v_\chi v_{S_1}}{\sqrt{2}\Lambda} \begin{pmatrix} 1+x & 0 & 0 \\ 0 & \omega^2 + x\omega & 0 \\ 0 & 0 & \omega + x\omega^2 \end{pmatrix} = \begin{pmatrix} m_{N_1} & 0 & 0 \\ 0 & m_{N_2} e^{i\beta_1} & 0 \\ 0 & 0 & m_{N_3} e^{i\beta_2} \end{pmatrix}, \\
M_R &= \begin{pmatrix} y_{2N} v_\varphi & y_{1N} v_\xi & -y_{1N} v_\xi \\ y_{1N} v_\xi & y_{2N} v_\varphi & y_{1N} v_\xi \\ -y_{1N} v_\xi & y_{1N} v_\xi & y_{2N} v_\varphi \end{pmatrix} \frac{v_{\sigma_3} v_{\sigma_1}^2 v_{\sigma_2}^4}{\Lambda^7} = \begin{pmatrix} \kappa_2 & \kappa_1 & -\kappa_1 \\ \kappa_1 & \kappa_2 & \kappa_1 \\ -\kappa_1 & \kappa_1 & \kappa_2 \end{pmatrix} \mu, \quad x = \frac{y_{1\chi}^{(L)} v_{S_1}}{y_{2\chi}^{(L)} v_{S_2}}, \\
\kappa_1 &= y_{1N}, \quad \kappa_2 = y_{2N} \frac{v_\varphi}{v_\xi}, \quad \mu = \frac{v_{\sigma_3} v_{\sigma_1}^2 v_{\sigma_2}^4 v_\xi}{\Lambda^7}.
\end{aligned} \tag{24}$$

The light active masses arise from an inverse seesaw (ISS) mechanism and the physical neutrino mass matrices are:

$$M_\nu^{(1)} = M_{\nu D} (M_\chi^T)^{-1} M_R M_\chi^{-1} M_{\nu D}^T, \tag{25}$$

$$M_\nu^{(2)} = -\frac{1}{2} (M_\chi + M_\chi^T) + \frac{1}{2} M_R, \quad M_\nu^{(3)} = \frac{1}{2} (M_\chi + M_\chi^T) + \frac{1}{2} M_R, \tag{26}$$

where $M_\nu^{(1)}$ is the light active neutrino mass matrix whereas $M_\nu^{(2)}$ and $M_\nu^{(3)}$ are the exotic Dirac neutrino mass matrices. The physical neutrino spectrum is composed of three light active neutrinos and six pseudo-Dirac exotic neutrinos, with masses $\sim \pm v_\chi \sim \mathcal{O}(10)$ TeV and a small splitting $\sim \mu$.

Sterile neutrinos can be produced in pairs at the Large Hadron Collider (LHC) through Drell-Yan annihilation, mediated by a heavy Z' gauge boson. These sterile neutrinos mix with the light active neutrinos, enabling their decay into Standard Model (SM) particles. As a result, the final decay products include an SM-charged lepton and a W gauge boson. Therefore, an excess of events in the dilepton final states, surpassing the SM background, could serve as a potential signature of this model at the LHC. Investigations into inverse seesaw neutrino signatures at colliders, as well as the production of heavy neutrinos at the LHC, have been conducted in, for example, in [126–131]. A thorough investigation of the collider implications of our model is beyond the scope of this work and will be explored in future research.

Thus, the mass matrix for light active neutrinos reads:

$$\begin{aligned}
M_\nu^{(1)} &= \begin{pmatrix} \kappa_2 a^2 - 2\kappa_1 ab + \kappa_2 b^2 & ab\kappa_1 - b\kappa_1 - b^2\kappa_2 - a\kappa_1 & a\kappa_1 + b\kappa_1 - a^2\kappa_2 + ab\kappa_1 \\ ab\kappa_1 - b\kappa_1 - b^2\kappa_2 - a\kappa_1 & \kappa_2 b^2 + 2\kappa_1 b + \kappa_2 & a\kappa_1 - \kappa_2 - b\kappa_1 - ab\kappa_1 \\ a\kappa_1 + b\kappa_1 - a^2\kappa_2 + ab\kappa_1 & a\kappa_1 - \kappa_2 - b\kappa_1 - ab\kappa_1 & \kappa_2 a^2 - 2\kappa_1 a + \kappa_2 \end{pmatrix} m_\nu, \\
m_\nu &= \frac{x_\rho^2 v_\rho^2 v_\eta^2 v_{\sigma_1}^4}{2 \left(y_\chi^{(L)}\right)^2 (1+x)^2 v_\chi^2 v_{S_1}^2 \Lambda^4} \mu, \quad a = \frac{1+x}{\omega^2 + x\omega}, \quad b = \frac{1+x}{\omega + x\omega^2}.
\end{aligned} \tag{27}$$

The light active neutrino mass matrix $M_\nu^{(1)}$ is diagonalized as follows:

$$R_\nu^T M_\nu^{(1)} R_\nu = \begin{pmatrix} 0 & 0 & 0 \\ 0 & m_2 & 0 \\ 0 & 0 & m_3 \end{pmatrix}, \quad R_\nu = \begin{pmatrix} \frac{1}{\sqrt{3}} & -\frac{1}{\sqrt{2}} & \frac{1}{\sqrt{6}} \\ \frac{1}{\sqrt{3}} & 0 & \frac{-2}{\sqrt{6}} \\ \frac{1}{\sqrt{3}} & \frac{1}{\sqrt{2}} & \frac{1}{\sqrt{6}} \end{pmatrix} \begin{pmatrix} 1 & 0 & 0 \\ 0 & \cos \theta & \sin \theta e^{-i\phi} \\ 0 & -\sin \theta e^{i\phi} & \cos \theta \end{pmatrix}, \tag{28}$$

and the light active neutrino masses are:

$$m_1 = 0, \tag{29}$$

$$m_2 = \frac{1}{2} A + \frac{1}{2} B - \frac{1}{2} \sqrt{A^2 - 2AB + B^2 + 4C^2}, \tag{30}$$

$$m_3 = \frac{1}{2} A + \frac{1}{2} B + \frac{1}{2} \sqrt{A^2 - 2AB + B^2 + 4C^2}. \tag{31}$$

Observable	Model value	Neutrino oscillation global fit values (NH)			
		Best fit $\pm 1\sigma$ [3]	Best fit $\pm 1\sigma$ [132]	3σ range [3]	3σ range [132]
Δm_{21}^2 [10^{-5}eV^2]	7.51 ± 0.60	$7.50^{+0.22}_{-0.20}$	$7.42^{+0.21}_{-0.20}$	$6.94 - 8.14$	$6.82 - 8.04$
Δm_{31}^2 [10^{-3}eV^2]	2.55 ± 0.21	$2.55^{+0.02}_{-0.03}$	$2.517^{+0.026}_{-0.028}$	$2.47 - 2.63$	$2.435 - 2.598$
$\theta_{12}^{(\ell)}$ ($^\circ$)	33.4495 ± 2.1648	34.3 ± 1.0	$33.44^{+0.77}_{-0.74}$	$31.4 - 37.4$	$31.27 - 35.86$
$\theta_{13}^{(\ell)}$ ($^\circ$)	8.54137 ± 0.26299	$8.58^{+0.11}_{-0.15}$	8.57 ± 0.12	$8.13 - 8.92$	$8.20 - 8.93$
$\theta_{23}^{(\ell)}$ ($^\circ$)	49.04 ± 2.05	$48.79^{+0.93}_{-1.25}$	$49.2^{+0.9}_{-1.2}$	$41.20 - 51.33$	$40.1 - 51.7$
$\delta_{\text{CP}}^{(\ell)}$ ($^\circ$)	-87.1246 ± 7.7968	216^{+41}_{-25}	197^{+27}_{-24}	$128 - 359$	$120 - 369$

Table IV: Model and experimental values of the neutrino mass-squared differences, leptonic mixing angles, and the CP-violating phase. Experimental values are taken from Refs. [3, 132].

where:

$$\begin{aligned}
A &= \left(2\kappa_2 a^2 - 2\kappa_1 ab - 2\kappa_1 a + \frac{1}{2}\kappa_2 b^2 - \kappa_1 b + \frac{1}{2}\kappa_2 \right) m_\nu, \\
B &= \left(\frac{3}{2}\kappa_2 b^2 + 3\kappa_1 b + \frac{3}{2}\kappa_2 \right) m_\nu, \\
C &= \left[-\frac{1}{2}\sqrt{3}(b-1)(\kappa_2 - 2a\kappa_1 + b\kappa_2) \right] m_\nu
\end{aligned}$$

and

$$\tan(2\theta) \equiv t_{2\theta} = \frac{\sqrt{3}(b-1)((b+1)\kappa_2 - 2a\kappa_1)}{\kappa_2(-2a^2 + b^2 + 1) + 2\kappa_1((a+2)b + a)}. \quad (32)$$

Note that we consider only the normal neutrino mass hierarchy, which is favored over the inverted hierarchy by more than 3σ . For the normal neutrino mass hierarchy, the PMNS leptonic mixing matrix takes the form:

$$U = R_{\ell L}^\dagger R_\nu = \begin{pmatrix} \cos \alpha \cos \gamma & \frac{(\omega+2)(\sin \alpha \cos \gamma + \sin \gamma)}{\sqrt{6}} & \frac{\omega(\sin \alpha \cos \gamma - \sin \gamma)}{\sqrt{2}} \\ \sin \alpha & -\frac{(\omega+2)\cos \alpha}{\sqrt{6}} & -\frac{\omega \cos \alpha}{\sqrt{2}} \\ -\omega \cos \alpha \sin \gamma & \frac{(\omega-1)(\cos \gamma - \sin \alpha \sin \gamma)}{\sqrt{6}} & \frac{(\omega+1)(\sin \alpha \sin \gamma + \cos \gamma)}{\sqrt{2}} \end{pmatrix} \begin{pmatrix} 1 & 0 & 0 \\ 0 & \cos \theta & \sin \theta e^{-i\phi} \\ 0 & -\sin \theta e^{i\phi} & \cos \theta \end{pmatrix}. \quad (33)$$

The charged lepton masses, the neutrino mass squared splittings, i.e. Δm_{21}^2 and Δm_{31}^2 , leptonic mixing angles $\theta_{12}^{(\ell)}$, $\theta_{23}^{(\ell)}$, $\theta_{13}^{(\ell)}$ and the Dirac leptonic CP violating phase are well reproduced for the following values of the lepton sector parameters:

$$\begin{aligned}
a_1^{(\ell)} &\simeq 0.427, & a_2^{(\ell)} &\simeq 1.026, & a_3^{(\ell)} &\simeq 0.882, \\
A &\simeq 31.65 \pm 3.12 \text{ meV}, & B &\simeq 27.46 \pm 2.24 \text{ meV}, & C &\simeq 20.79 \pm 9.31 \text{ meV}, \\
\theta &\simeq (-107.89 \pm 3.33)^\circ, & \phi &\simeq (-29.83 \pm 2.07)^\circ, \\
\alpha &\simeq (-21.63 \pm 1.15)^\circ, & \gamma &\simeq (-337.70 \pm 8.85)^\circ,
\end{aligned} \quad (34)$$

or

$$\kappa_1 = -0.655001, \quad \kappa_2 = 0.726924, \quad x = -0.695083 + 0.718929i. \quad (35)$$

As shown in Table IV, our model is consistent with the experimental data on lepton masses and mixing. It is worth mentioning that our model allows to successfully reproduce the experimental values of the six physical observables of the neutrino sector with only four effective parameters. Analogously to the quark sector (see Eq. (18)), the fit of the leptonic sector is obtained by minimizing the function χ_ℓ^2 , which reproduces the values in Table IV and the best-fit point from Eqs. (34) and (35).

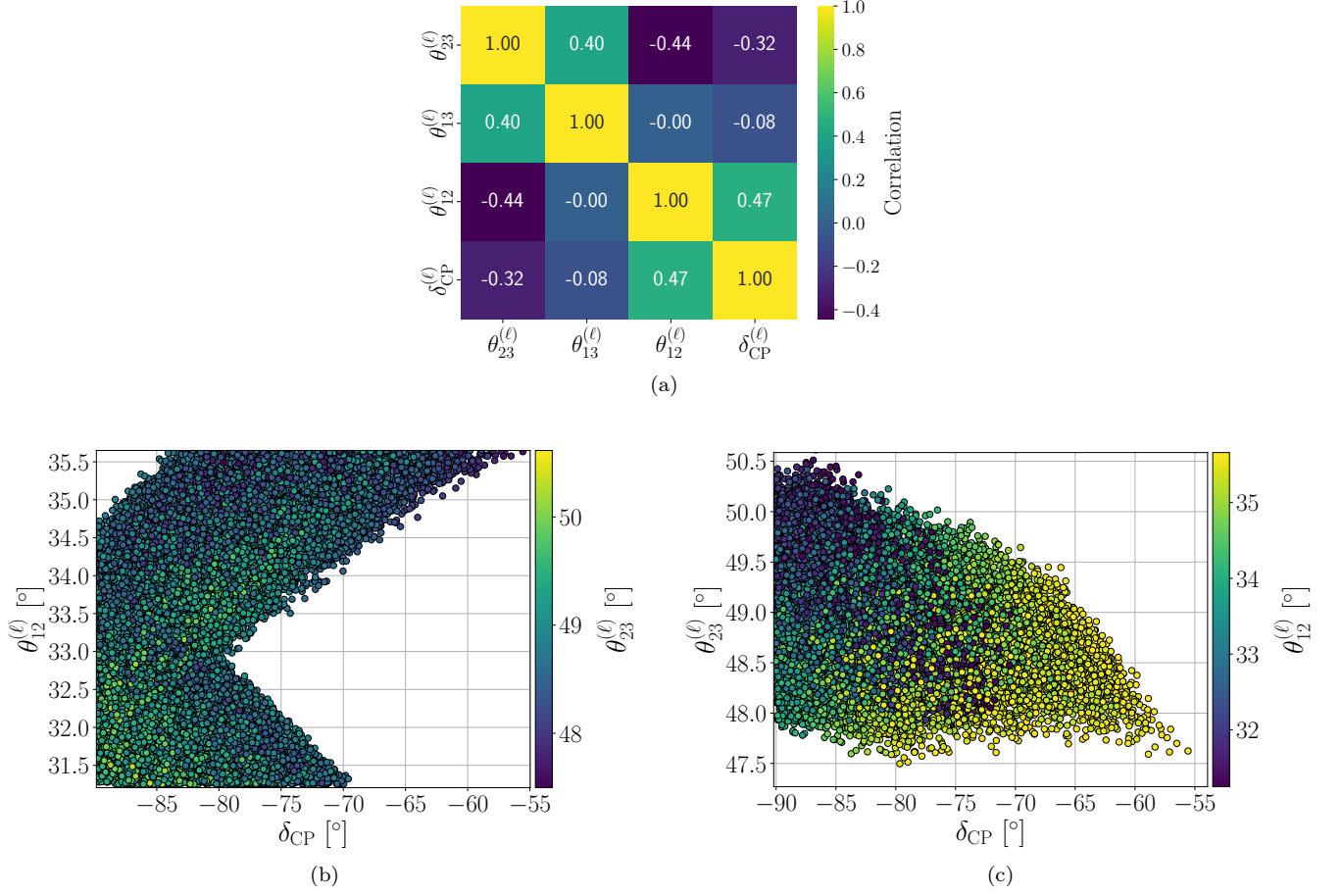


Figure 4: (a) Correlation heat-map: Illustrated the pairwise correlations between lepton mixing angle and the Dirac CP-violating phase. The intensity of color represents the strength of the correlation. (b) Correlation between the solar mixing parameter and the leptonic Dirac CP phase, where the range of colors represents the correlation for the atmospheric mixing parameter our model. (c) Explored the correlation between the atmospheric mixing parameters and the Dirac CP-violating phase.

Figure 4 illustrates the correlations among the lepton mixing parameters and the Dirac CP-violating phase. Panel (a) presents a heat-map, revealing the strongest correlations between the mixing angles $\theta_{23}^{(\ell)}$ and $\theta_{13}^{(\ell)}$. In contrast, the correlation with the phase $\delta_{CP}^{(\ell)}$ is weaker, as indicated by the lower intensity in the values of the heat-map. Panel (b) displays the correlation between the solar mixing parameter $\theta_{12}^{(\ell)}$ and the Dirac CP-violating phase $\delta_{CP}^{(\ell)}$, which aligns with their 3σ experimentally allowed ranges. Here the color range represents the correlation intensity for the atmospheric mixing parameter. Finally, panel (c) provides a similar visualization to panel (b), but focused on the atmospheric mixing parameter and the Dirac phase. This analysis is crucial for understanding the experimental constraints arising from the lepton mixing in our model.

Another observable predicted by our models is the effective Majorana neutrino mass parameter associated with neutrinoless double-beta decay ($0\nu\beta\beta$). This process plays a pivotal role in investigating the Majorana nature of neutrinos, as it involves a nuclear decay that emits two electrons without any accompanying neutrinos. Its experimental observation would imply that neutrinos are Majorana fermions, violating the lepton number by two units and thereby pointing toward physics beyond the Standard Model.

The key parameter describing the amplitude of this process is the effective Majorana mass, m_{ee} , given by

$$m_{ee} = \left| \sum_i U_{ei}^2 m_{\nu_i} \right|, \quad (36)$$

where U_{ei} are the elements of the PMNS matrix and m_{ν_i} are the masses of the light active neutrinos. The theoretical

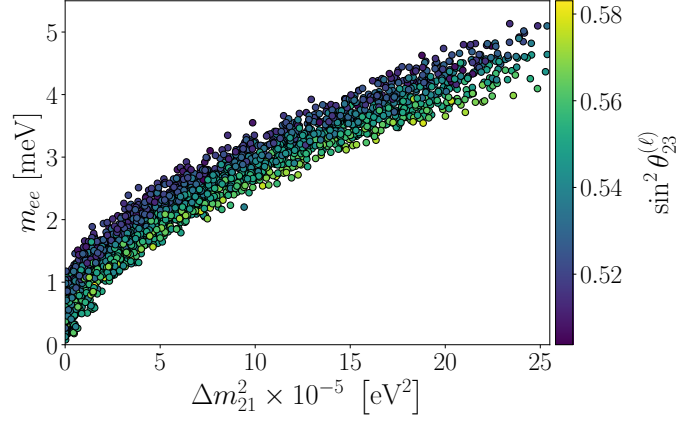


Figure 5: Correlation between the squared neutrino mass difference Δm_{21}^2 and the effective Majorana neutrino mass parameter m_{ee} . The color scale represents the variation of the leptonic mixing parameter $\sin^2 \theta_{23}^{(\ell)}$, highlighting its influence on the distribution of m_{ee} .

estimation of this value depends on the neutrino mass hierarchy.

In Figure 5 illustrates the correlation between the effective Majorana neutrino mass parameter m_{ee} and the neutrino mass squared difference Δm_{21}^2 , the color scale representing the leptonic mixing parameter $\sin^2 \theta_{23}^{(\ell)}$. The predictions in this work are derived under the assumption of a normal neutrino mass hierarchy and are consistent with the experimentally allowed ranges for neutrino oscillation parameters. The effective Majorana neutrino mass parameter m_{ee} is predicted to lie in the range $0.1 \text{ meV} \lesssim m_{ee} \lesssim 5.0 \text{ meV}$, which is well below the current experimental upper bound of $m_{ee} \lesssim 50 \text{ meV}$ set by KamLAND-Zen [133] based on the non-observation of the decay of $0\nu\beta\beta$ for ^{136}Xe , with a half-life constraint of $T_{1/2}^{0\nu} > 2.0 \times 10^{26} \text{ yr}$ at the confidence level 90%. Furthermore, our predictions are consistent with cosmological bounds from the Planck collaboration, which constrain the sum of neutrino masses to $\sum m_{\nu_i} < 0.115 \text{ eV}$ at 95% confidence level [4], taking into account our scenario of Eq. (34), we obtain a value in the following range $0.01 \text{ eV} \lesssim \sum m_{\nu_i} \lesssim 0.06 \text{ eV}$. The results presented here provide a robust framework to explore the parameter space of m_{ee} within the context of normal hierarchy, highlighting the complementarity of neutrinoless double beta decay experiments and cosmological observations in probing the fundamental properties of neutrinos.

V. HIGGS AND GAUGE BOSONS

The model consists of 8 electroweak gauge bosons W_μ^a of the $SU(3)_L$ gauge group and X_μ of $U(1)_X$. The corresponding covariant derivative is:

$$D_\mu = \partial_\mu - igT^a W_\mu^a - ig_X X T^9 X_\mu, \quad (37)$$

where T^a are generators of the $SU(3)_L$ group, $T_9 = I/\sqrt{6}$, X is the $U(1)_X$ charge, and

$$\frac{g_X}{g} = \frac{3\sqrt{2}t_W}{\sqrt{3-t_W^2}}, \quad (38)$$

with $t_W = \frac{\sin \theta_W}{\cos \theta_W}$, θ_W is the Weinberg angle which is satisfied: $\sin^2 \theta_W \simeq 0.231$.

After symmetry breaking, the model contains SM gauge bosons, including the massless photon A_μ with their field given by

$$A_\mu = s_W W_{3\mu} - \frac{s_W}{\sqrt{3}} W_{8\mu} + \frac{\sqrt{1+2c_{2W}}}{\sqrt{3}} X_\mu, \quad (39)$$

as well as two neutral weak gauge bosons

$$Z_\mu = c_W W_{3\mu} - t_W \left(-\frac{s_W}{\sqrt{3}} W_{8\mu} + \frac{\sqrt{1+2c_{2W}}}{\sqrt{3}} X_\mu \right), \quad Z'_\mu = \frac{\sqrt{1+2c_{2W}}}{\sqrt{3}s_W} W_{8\mu} + \frac{t_W}{\sqrt{3}} X_\mu, \quad (40)$$

with $c_W = \cos \theta_W$, $s_W = \sin \theta_W$. In the former expressions, the neutral currents of Z_μ coincide with the weak neutral current of the SM. However, in the model considered, the physical fields $Z_{1\mu}, Z_{2\mu}$ are defined

$$Z_{1\mu} = c_z Z_\mu - s_z Z'_\mu, \quad Z_{2\mu} = s_z Z_\mu + c_z Z'_\mu \quad (41)$$

where $s_z \equiv \sin \theta_z$, $c_z \equiv \cos \theta_z$, $c_{331} = \cos \theta_{331}$, $s_{331} = \sin \theta_{331}$ and

$$\tan 2\theta_z = -\frac{2c_W \sqrt{3-t_W^2} v_\rho^2}{4c_W^4 v_\chi^2 + c_W^2 (t_W^2 - 3) v_\rho^2 + v_\rho^2}, \quad \tan \theta_{331} = -3\sqrt{2} \frac{g}{g_X}. \quad (42)$$

In the limit $\frac{v_\rho^2}{v_\chi^2} \sim O(\lambda^6) \simeq 0$, we have

$$m_{Z_1}^2 \simeq \frac{m_W^2}{c_W^2}, \quad m_{Z_2}^2 \simeq \frac{g^2 v_\chi^2}{3-t_W^2}. \quad (43)$$

The single-charged gauge bosons Z and W^\pm .

$$W_\mu^\pm \equiv \frac{W_\mu^1 \mp iW_\mu^2}{\sqrt{2}}, \quad m_W = \frac{g v_\rho}{2}. \quad (44)$$

There are four new heavy-complex gauge bosons

$$X_\mu^0 \equiv \frac{W_\mu^4 - iW_\mu^5}{\sqrt{2}}, \quad Y_\mu^\pm \equiv \frac{W_\mu^6 \mp iW_\mu^7}{\sqrt{2}}, \quad (45)$$

with their masses

$$m_X = \frac{g v_\chi}{2}, \quad m_Y^2 = m_X^2 + m_W^2. \quad (46)$$

For user convenience, we provide the basis transformation matrix of the neutral gauge bosons, defined as

$$\begin{pmatrix} X_\mu \\ W_\mu^3 \\ W_\mu^8 \end{pmatrix} = C_{zz'} \begin{pmatrix} A_\mu \\ Z_{1\mu} \\ Z_{2\mu} \end{pmatrix}, \quad C_{zz'} = \begin{pmatrix} c_W s_{331} & c_{331} s_z - c_z s_{331} s_W & c_{331} c_z + s_{331} s_W s_z \\ s_W & c_W c_z & -c_W s_z \\ c_{331} c_W & -c_{331} c_z s_W - s_{331} s_z & c_{331} s_W s_z - c_z s_{331} \end{pmatrix}, \quad (47)$$

For the details of the Higgs potential, see Appendix B. The model contains a singly charged Higgs boson and a SM-like Higgs boson found by LHC.

VI. FCNCS

Since the quark generations are non-universal under the $SU(3)_L \times U(1)_X$ gauge symmetry, the corresponding tree-level flavor-changing neutral currents (FCNCS) must also be non-universal. Indeed, considering the interaction of neutral gauge bosons with fermions, we have:

$$\mathcal{L}_{N.C} = -g \bar{f} \gamma^\mu \left\{ T_3 W_{3\mu} + T_8 A_{8\mu} + \frac{t}{\sqrt{6}} (Q - T_3 - \beta T_8) B_\mu \right\} f, \quad (48)$$

where f runs over all fermion multiplets. The FCNCS associate only with T_8 for ordinary quarks, the revenant interactions are

$$\begin{aligned} \mathcal{L}_{N.C} &\supset -g \bar{q}_{aL} \gamma^\mu T_8 q_{aL} \left(A_{8\mu} - \frac{\beta}{\sqrt{6}} t B_\mu \right) = -\frac{g\sqrt{3}}{\sqrt{3-t_W^2}} \bar{q}_{aL} \gamma^\mu T_8 q_{aL} Z'_\mu \\ &= -\frac{g\sqrt{3}}{\sqrt{3-t_W^2}} \bar{q}_L \gamma^\mu T_q q_L (-s_z Z_{1\mu} + c_z Z_{2\mu}), \end{aligned} \quad (49)$$

with $T_q = \frac{1}{2\sqrt{3}}\text{Diag}(1, -1, -1)$ for gauge states $q = u_L = (u_{1L}, u_{2L}, u_{3L})^T$ or $q = d_L = (d_{1L}, d_{2L}, d_{3L})^T$. The gauge states are related to the mass eigenstates by $u_{L,(R)} = V_{u_L(u_R)} u'_{L,(R)}$ and $d_{L,(R)} = V_{d_L(u_R)} d'_{L,(R)}$. The CKM matrix is given by $V_{\text{CKM}} = V_{u_L}^\dagger V_{d_L}$. Due to the specific form of the quark mass matrix presented in Eq. (16), the mixing matrix V_{d_L} is simply the identity matrix, specifically $V_{d_L} = \text{Diag}(1, 1, 1)$. This indicates that $V_{u_L}^\dagger$ is equivalent to the CKM matrix, which means $V_{u_L}^\dagger = V_{\text{CKM}}$. Consequently, transitioning to the mass eigenstates results in tree-level FCNCs only happen in u -quark sector

$$\begin{aligned} \mathcal{L}_{\text{FCNC}} &= -\frac{g}{\sqrt{3-t_W^2}} \left\{ (V_{\text{CKM}}^T)_{1i} (V_{\text{CKM}}^\dagger)_{1j} \right\} \bar{u}'_{iL} \gamma^\mu u_{jL} (-s_z Z_{1\mu} + c_z Z_{2\mu}) \\ &= \vartheta_{ij} \bar{u}'_{iL} \gamma^\mu u_{jL} (-s_z Z_{1\mu} + c_z Z_{2\mu}), \end{aligned} \quad (50)$$

with

$$\vartheta_{ij} = -\frac{g}{\sqrt{3-t_W^2}} \left\{ (V_{\text{CKM}}^T)_{1i} (V_{\text{CKM}}^\dagger)_{1j} \right\}. \quad (51)$$

Additional, the model also contains the scalar FCNCs associated to neutral scalars content in the triplet scalar Higgs. Two physical states carrying both even Z_2^L and CP charges, (h_1, h_2) , relates to two scalar components (ξ_ρ, ξ_χ) by unitary rotation matrix as follows

$$(\xi_\rho, \xi_\chi)^T = \mathcal{R}(h_1, h_2)^T. \quad (52)$$

There is a tiny mixing between the two components ξ_ρ and ξ_χ because ξ_ρ is a doublet of the $SU(2)_L$ group, while ξ_χ is a singlet of this group. This implies that the matrix elements $\mathcal{R}_{11} \simeq \mathcal{R}_{22} \simeq 1$ and $\mathcal{R}_{12} \simeq \mathcal{R}_{21} \sim \frac{v_\rho}{v_\chi} \sim \lambda^2$. After changing to the physical states, we obtain the scalar FCNCs associated with the CP-even scalar Higgs:

$$\mathcal{L}_{\text{FCNC}}^{\text{scalar}} = \Gamma_{\alpha\alpha'}^{h_i} \bar{u}_{\alpha L} u_{\alpha' R} h_i + h.c. \quad (53)$$

with

$$\Gamma_{\alpha\alpha'}^{h_i} = \frac{m_{u'_\alpha}}{v_\rho} (\mathcal{R}_{1i} + \mathcal{R}_{2i} \lambda^2 - 1) (V_{\text{CKM}}^T)_{1\alpha} (V_{\text{CKM}}^\dagger)_{1\alpha'} \simeq \frac{m_{u'_\alpha}}{v_\rho} \lambda^4 (V_{\text{CKM}}^T)_{1\alpha} (V_{\text{CKM}}^\dagger)_{1\alpha'}. \quad (54)$$

The coefficients given by Eqs. (51) and (54) show that $\vartheta_{ij} \gg \Gamma_{ij}$. The $\tan 2\theta_z \simeq \lambda^4$. These mean that the FCNCs associated with the neutral scalars and $Z_{1\mu}$ are suppressed compared to those of the new neutral gauge bosons $Z_{2\mu}$. Hence, we may omit the FCNC contributions related to the neutral Higgs bosons and $Z_{1\mu}$ in the following studies.

We want to emphasize that, unlike previous studies, our model predicts the existence of tree-level FCNCs primarily associated with the u -quark. This feature is shown in Figure 6, where the Feynman diagram depicts FCNCs in the up-quark sector, mediated by the neutral bosons Z_μ and Z'_μ . Consequently, our model is not tightly constrained by B-meson oscillations but only by D-meson oscillations. At tree level, the effective Lagrangian for the D-meson oscillation process is as follows:

$$\mathcal{L}_{Z'_{\text{eff}}^{D_0-\bar{D}_0}} = \mathcal{G}' \frac{m_{Z_1}^2}{m_{Z_2}^2} |(V_{\text{CKM}})_{11} (V_{\text{CKM}}^*)_{21}|^2 |\bar{u}'_{1L} \gamma^\mu u'_{2L}|^2, \quad (55)$$

where $\mathcal{G}' = \frac{4\sqrt{2}G_F}{1+4c_W^2}$, with G_F being the Fermi constant. This effective Lagrangian contributes to the mass splittings Δm_D between neutral mesons D_0 and \bar{D}_0 as follows:

$$\Delta m_D = \mathcal{G}' \frac{m_{Z_1}^2}{m_{Z_2}^2} |(V_{\text{CKM}})_{11} (V_{\text{CKM}}^*)_{21}|^2 f_D^2 B_D \eta_D m_D. \quad (56)$$

Values for the bag parameter B_D , decay constant f_D , QCD correction factor η_D , and the D-meson mass are taken from [134]:

$$\sqrt{B_D} f_D = 187 \text{MeV}, \quad \eta_D = 0.57, \quad m_D = (1865 \pm 0.0005) \text{MeV}. \quad (57)$$

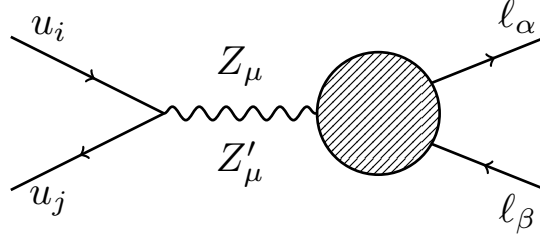


Figure 6: Feynman diagram representing flavor-changing neutral currents (FCNC) in the up-quark sector. The vertex involves the neutral bosons Z_μ and Z'_μ .

The SM predicted value for Δm_D is

$$(\Delta m_D)_{\text{SM}} = 10^{-14} \text{MeV}, \quad (58)$$

while the experimental value is

$$(\Delta m_D)_{\text{exp}} = (6.25316_{-2.8962}^{+2.69873}) \times 10^{-12} \text{MeV}. \quad (59)$$

This means that the main contribution to the D-meson mass difference comes from the NP. From the experimental bound, we obtain the lower bound on the Z_2 -boson mass: $m_{Z_2} > 173 \text{TeV}$.

We would like to point out that if we organize the third quark family transform differently from the first two families under the symmetry group $SU(3)_c \times U(1)_L$, the NP contribution to the D-meson mass difference becomes proportional to $|(V_{\text{CKM}})_{13} (V_{\text{CKM}}^*)_{32}|^2$ instead of being proportional to $|(V_{\text{CKM}})_{11} (V_{\text{CKM}}^*)_{21}|^2$, as considered in the version considered. In this scenario, the constraint on the oscillation of D_0 and \bar{D}_0 results in a lower bound on the mass of the new neutral boson, which is approximately a few TeV.

Since the three lepton families transform identically under $SU(3)_c \times U(1)_L$, lepton FCNCs are forbidden at the tree level but occur at the loop level, as demonstrated in [135]. The model allows for lepton flavor violation (LFV) via one-loop penguin diagrams in meson decays, particularly in D-meson decays. The general four-fermion Hamiltonian describing the interaction for the process $u'_1 \rightarrow u'_2 l_\alpha^+ l_\beta^-$ can be expressed as follows:

$$\mathcal{H}_{\text{eff}} = \frac{4G_{\text{F}}}{\sqrt{2}} (C_9 O_9 + C_{10} O_{10}), \quad (60)$$

where

$$\begin{aligned} C_9 &\simeq \frac{2}{1 + 4c_W^2} \frac{4\pi^2}{e^2} \left(\frac{m_{Z_1}^2}{m_{Z_2}^2} \right) (V_{\text{CKM}})_{11} (V_{\text{CKM}}^*)_{12} (\bar{a}_l + \bar{a}_r), \\ C_{10} &\simeq \frac{2}{1 + 4c_W^2} \frac{4\pi^2}{e^2} \left(\frac{m_{Z_1}^2}{m_{Z_2}^2} \right) (V_{\text{CKM}})_{11} (V_{\text{CKM}}^*)_{12} (\bar{a}_l - \bar{a}_r). \end{aligned} \quad (61)$$

In our case, the expressions for $\bar{a}_{l(r)}$ are determined similarly to those for $a_{l(r)}$ given in [135]. In that work, they predicted $\text{Br}(Z \rightarrow \mu e) \sim 10 \times 10^{-12}$, which resulted in coefficient values of $a_{l(r)} \simeq 10^{-3}$. Combining this with the limit $m_{Z_2} > 173 \text{TeV}$, we can roughly estimate the Wilson coefficients $C_{10}, C_9 \sim 10^{-10}$. Due to these small values, we predict suppressed values for the branching ratios of charged lepton flavor violation in D-meson decays, well below the experimental upper bound reported in [136].

Due to the light-heavy neutrino mixing matrix elements, the model also yields the box diagrams for the transition $q_i \rightarrow q_j l_\alpha^+ l_\beta^-$. The internal lines can be either a light neutrino or heavy neutrino, and either the SM W_μ^\pm or new charged gauge bosons Y_μ^\pm . However, the contributions to the Wilson coefficients from the box diagrams are very small [137, 138]. Hence, we do not consider them in our work.

VII. LEPTON FLAVOR VIOLATING DECAYS $e_j \rightarrow e_i$

Based on the definition of the covariant derivative associated with the electroweak gauge group $SU(3)_L \times U(1)_X$, the charged gauge boson component V_μ^{CC} of the derivative D_μ associated in the model under consideration is given by:

$$V_\mu^{CC} \equiv \frac{1}{\sqrt{2}} \begin{pmatrix} 0 & W_\mu^+ & 0 \\ W_\mu^- & 0 & Y_\mu^- \\ 0 & Y_\mu^+ & 0 \end{pmatrix}. \quad (62)$$

Given that the one-loop contributions from neutral Higgs bosons, Z and Z' bosons involve couplings only to the SM charged lepton, we will ignore them in this work. Therefore, we will focus solely on the couplings of charged leptons to both heavy neutral leptons and charged gauged bosons, which are relevant for one-loop contributions to LFV decays. The calculation will be performed on the unitary gauge.

Left-handed charged leptons are transformed from the flavor basis $l_{iL,R}$ to the physical basis $e_{iL,R}$ using the matrix $R_{\ell L}$ from Eq. (20) $l_{iL} = R_{\ell L,ij} e_{jL}$ with $i, j = 1, 2, 3$. The neutrino mass matrix M_ν in Eq. (23) is diagonalized by the unitary matrix U_ν :

$$U_\nu^T M_\nu U_\nu = \hat{M}_\nu = \begin{pmatrix} \hat{m}_\nu & \mathbf{0}_{3 \times 9} \\ \mathbf{0}_{9 \times 3} & \hat{m}_N \end{pmatrix}, \quad (63)$$

where $\hat{m}_\nu = \text{diag}(m_{n_1}, m_{n_2}, m_{n_3})$ and $\hat{m}_N = \text{diag}(m_{n_4}, m_{n_5}, \dots, m_{n_9})$ are the diagonal masses matrices for the light and heavy Majorana neutrinos $n_L = (n_{1L}, n_{2L}, \dots, n_{9L})$, respectively. This implies the following relationship between flavor and physical states: $(\overline{\nu}_L^C \ \overline{\nu}_R \ \overline{N}_R) = \overline{n}_R U_\nu^T$ and $(\nu_L \ \nu_R^C \ N_R^C)^T = U_\nu n_L$. Due to the ISS condition $|m_D| \ll |M_\chi|$, the light neutrino mixing matrix R_ν from Eq. (33) is approximately equal to U_ν : $R_{\nu,ij} \simeq U_{\nu,ij}$ for all $i, j = 1, 2, 3$.

The rotation matrix U_ν from Eq. (63) is given by [139]:

$$U_\nu = \begin{pmatrix} R_\nu & R_1 R_M^{(2)} & R_2 R_M^{(3)} \\ -\frac{(R_1^\dagger + R_2^\dagger)}{\sqrt{2}} R_\nu & \frac{(1-S)}{\sqrt{2}} R_M^{(2)} & \frac{(1+S)}{\sqrt{2}} R_M^{(3)} \\ -\frac{(R_1^\dagger - R_2^\dagger)}{\sqrt{2}} R_\nu & \frac{(-1-S)}{\sqrt{2}} R_M^{(2)} & \frac{(1-S)}{\sqrt{2}} R_M^{(3)} \end{pmatrix}, \quad (64)$$

where the submatrices R_1 , R_2 and S are defined from the Eq. (24) as follows:

$$R_1 \simeq R_2 \simeq \frac{1}{\sqrt{2}} M_{\nu D}^* M_\chi^{-1}, \quad S = -\frac{1}{4} M_\chi^{-1} M_R, \quad (65)$$

and $R_M^{(2)}$, $R_M^{(3)}$ diagonalize the exotic neutrino matrices.

The covariant kinetic terms of L_{iL} give the following couplings of charged gauge bosons with leptons:

$$\begin{aligned} \mathcal{L}_{Vll} &= g \sum_{i=1}^3 \overline{L_{iL}} V_\mu^{CC} \gamma^\mu L_{iL} = \frac{g}{\sqrt{2}} \sum_{i=1}^3 \left(\overline{\nu_{iL}} \gamma^\mu l_{iL} W_\mu^+ + (\overline{\nu_{iR}})^C \gamma^\mu l_{iL} Y_\mu^+ \right) + H.c. \\ &= \frac{g}{\sqrt{2}} \sum_{a=1}^9 \sum_{i,j=1}^3 \left(\overline{n_a} \gamma^\mu U_{\nu,a,j}^\dagger R_{\ell L,ji} P_L e_i W_\mu^+ + \overline{n_a} \gamma^\mu U_{\nu,a,(j+3)}^\dagger R_{\ell L,ij} P_L e_i Y_\mu^+ \right) + H.c. \end{aligned} \quad (66)$$

with $P_L = (1 - \gamma_5)/2$.

Processes like $\mu \rightarrow e\gamma$ are crucial for probing beyond SM physics, including 3-3-1 models. Based on the developments presented in [140, 141], we explore the LFV processes arising from non-universal couplings of the standard charged leptons to the gauge bosons. In our model, LFV is directly linked to the masses and interactions of exotic neutrinos and their associated gauge bosons. Experimental limits, particularly MEG ones, impose stringent constraints on the parameter space of 3-3-1 models. Future experiments, conversion in aluminum and titanium nuclei, will further refine these constraints and provide insights into the scale of new physics.

The analytic expression for the branching ratio (Br) for the decay of $e_i \rightarrow e_j \gamma$ ($m_{e_i} > m_{e_j}$) is given by [140, 144–147]:

$$\text{Br}(e_i \rightarrow e_j \gamma) = \frac{12\pi^2}{G_F^2} |\Gamma_{ij}|^2 \times \text{Br}(e_i \rightarrow e_j \bar{\nu}_j \nu_i), \quad (67)$$

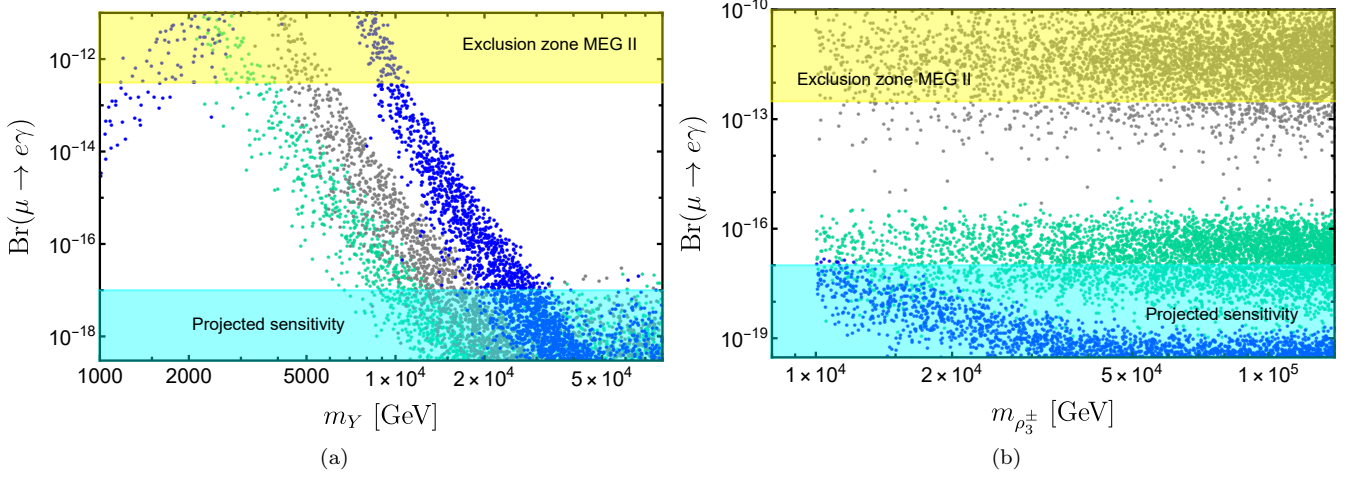


Figure 7: Branching ratio for $\mu \rightarrow e\gamma$ as a function of the mass of the gauge boson Y (panel a) and the charged scalar ρ_3^\pm (panel b). The upper shaded region corresponds to an area excluded by the MEG II experiment [142] and the lower shaded region corresponds to the expected sensitivities of the next generation of experiments using aluminium as targets [143].

where Γ_{ij} represents the one-loop contribution from virtual charged gauge bosons and Majorana neutrinos in the loop diagrams. The contribution can be expressed as: $\Gamma_{ij} = \Gamma_{ij}^W + \Gamma_{ij}^Y + \Gamma_{ij}^{\rho_3^\pm}$, where:

$$\begin{aligned}\Gamma_{ij}^W &= -\frac{eg^2}{32\pi^2 m_W^2} \sum_{k=1}^9 \sum_{a,b=1}^3 (R_{lL}^*)_{ib} (U_\nu^*)_{bk} (R_{lL})_{ja} (U_\nu)_{ak} \mathcal{F}\left(\frac{m_{n_k}^2}{m_W^2}\right), \\ \Gamma_{ij}^Y &= -\frac{eg^2}{32\pi^2 m_Y^2} \sum_{k=1}^9 \sum_{a,b=1}^3 (R_{lL}^*)_{ib} (U_\nu^*)_{(b+3)k} (R_{lL})_{ja} (U_\nu)_{(a+3)k} \mathcal{F}\left(\frac{m_{n_k}^2}{m_Y^2}\right), \\ \Gamma_{ij}^{\rho_3^\pm} &= \frac{e^2}{2} \sum_{k=1}^9 \frac{z_{kj}^* z_{ki}}{(4\pi)^2} \frac{1}{m_{\rho_3^\pm}^2} \mathcal{G}\left(\frac{m_{n_k}^2}{m_{\rho_3^\pm}^2}\right)\end{aligned}\quad (68)$$

with

$$z_{ki} = \sum_{r=1}^3 \sum_{s=1}^3 y_{\rho_3^{\pm}}^{rs} (R_{lL}^\dagger)_{ir} (\tilde{U}_\nu)_{sk}, \quad (69)$$

and the loop functions $\mathcal{F}(z)$ and $\mathcal{G}(z)$ are defined as:

$$\begin{aligned}\mathcal{F}(z) &= 2(z+2)\mathcal{I}_3(z) - 2(2z-1)\mathcal{I}_2(z) + 2z\mathcal{I}_1(z) + 1, \\ \mathcal{G}(z) &= \frac{1 - 6z + 3z^2 + 2z^3 - 6z^2 \log z}{6(1-z)^4},\end{aligned}\quad (70)$$

$$\mathcal{I}_n(z) = \frac{1}{4} \int_0^1 \frac{t^n}{z(t-1) - t} dt. \quad (71)$$

An additional LFV process is the $\mu \rightarrow e$ conversion in nuclei. The conversion rate is defined as the ratio [147, 148]

$$\text{CR}(\mu - e) = \frac{\Gamma(\mu^- + \text{Nucleus}(A, Z) \rightarrow e^- + \text{Nucleus}(A, Z))}{\Gamma(\mu^- + \text{Nucleus}(A, Z) \rightarrow \nu_\mu + \text{Nucleus}(A, Z - 1))}, \quad (72)$$

where A is the mass number and Z is the atomic number of the nucleus.

In 331 models, the μ - e conversion is more sensitive than the decay $\mu \rightarrow e\gamma$, with the sensitivity restricted by approximately two orders of magnitude. Future experiments are expected to significantly improve these sensitivities,

reaching an estimated limit of 10^{-17} for experiments using aluminum. Taking the above into account, the estimation of the μ - e conversion can be made using the following relation [147], which approximates the connection between the conversion in aluminum nuclei and the decay rate $\mu \rightarrow e\gamma$:

$$\text{CR}(\mu^- \text{Al} \rightarrow e^- \text{Al}) \approx \frac{1}{350} \text{Br}(\mu \rightarrow e\gamma). \quad (73)$$

The dominance of the photon in the μ - e conversion guarantees the applicability of the previous relation; this is fulfilled in our case, because at tree level we do not have neutral scalars that change flavor.

Figure 7 displays the model predictions for the branching ratio $\text{Br}(\mu \rightarrow e\gamma)$ as a function of the exotic gauge boson mass m_Y and the charged scalar mass $m_{\rho_3^\pm}$. In panel (a) the color-coded points represent different exotic neutrino mass values: green for 1 TeV, gray for 2 TeV, and blue for 5 TeV, whereas in panel (b) the color-coded point represent different mass ranges of the exotic gauge boson Y . The yellow shaded region, constrained by the MEG II experiment's limit of $\text{Br}(\mu \rightarrow e\gamma) < 3.1 \times 10^{-13}$ [142], excludes certain parameter space regions. The cyan shaded region indicates the projected sensitivity of future experiments like μ - e conversion in titanium and aluminum nuclei, with a sensitivity of $\text{CR}(\mu^- \text{Al} \rightarrow e^- \text{Al}) \lesssim 10^{-17}$ [143]. Numerically, the Yukawa couplings $y_{\rho_3^-}$ arising from the Dirac block fluctuate within the range 0.01 to 0.1, and the relevant couplings are given by $x_\rho = 1.99$ and $y_{1\chi}^{(L)} = 1.92$, which directly affect the magnitude of the contributions from gauge bosons and exotic neutrinos to LFV processes, since they control the active-sterile neutrino mixing angles given by Eq. (65), which determine the couplings of the neutrinos with SM charged leptons and charged gauge bosons, then giving rise to charged lepton flavor violating processes.

The most stringent limits for LFV arise from muon decay measurements, particularly from $\mu \rightarrow e\gamma$. The latest experimental results impose a strict upper limit on the branching ratio of this process, represented in the upper part of the plot in Figure 7.

In Figure 8, the correlations between the branching ratios $\text{Br}(\mu \rightarrow e\gamma)$ and $\text{Br}(\tau \rightarrow e\gamma)$, as well as between $\text{Br}(\tau \rightarrow \mu\gamma)$ and the conversion rate $\text{CR}(\mu \text{Al} \rightarrow e \text{Al})$, are shown. In panel (a), the relationship between $\text{Br}(\mu \rightarrow e\gamma)$ and $\text{Br}(\tau \rightarrow e\gamma)$ is illustrated through a color gradient that indicates the values of $\text{Br}(\tau \rightarrow \mu\gamma)$. This panel provides insight into how lepton flavor violation in the muon and tau decays correlates with the respective branching ratios of these processes. In panel (b), the correlation between $\text{Br}(\tau \rightarrow \mu\gamma)$ and the conversion rate $\text{CR}(\mu^- \text{Al} \rightarrow e^- \text{Al})$ is presented, with a color gradient reflecting the values of the gauge boson mass m_Y . In panel (c), the correlation between $\text{Br}(\tau \rightarrow e\gamma)$ and the conversion rate $\text{CR}(\mu^- \text{Al} \rightarrow e^- \text{Al})$ is presented, with a color gradient reflecting the values of the charged scalar mass $m_{\rho_3^\pm}$. This offers a direct indication of the dependence of the conversion rates on the mass of the new gauge boson in our model. The yellow shaded region in both panels marks the exclusion zone from the experimental limits set by the MEG II experiment [142].

In Table V, we present numerical cases for the heavy neutrino masses m_{n_4} to m_{n_9} , also include the mass of the gauge boson m_Y and the charged scalar mass $m_{\rho_3^\pm}$, both expressed in TeV, the corresponding branching ratios for processes $\mu \rightarrow e\gamma$, $\tau \rightarrow e\gamma$ and $\tau \rightarrow \mu\gamma$ and the estimated conversion rate $\text{CR}(\mu^- \text{Al} \rightarrow e^- \text{Al})$. These values provide insight into the correlations between the LFV processes and the masses of the heavy neutrinos and gauge bosons within the context of our model.

In what follows we provide a qualitative discussion about the implications of our model in the muon anomalous magnetic moment. It is important to note that the muon anomalous magnetic moment receives several contributions. These include effects from the virtual exchange of heavy neutral and electrically charged gauge bosons paired with their corresponding charged and neutral leptons, as well as contributions from electrically charged scalars and neutrinos. However, these additional contributions are negligible due to the highly suppressed mixing angle between the neutral CP-even component of the $SU(3)_L$ scalar triplet ρ and the other CP-even scalars. As for the contribution from electrically charged scalars and light active neutrinos, our numerical analysis shows that it can account for the observed magnitude of the muon $g-2$ anomaly when the charged scalars are lighter than 400 GeV. Nevertheless, this contribution is negative and therefore cannot explain the correct sign of the anomaly. In order to successfully reproduce the $g-2$ muon anomaly in our model, its fermion sector has to be enlarged by the inclusion of charged vector like leptons, transforming as singlets under the $SU(3)_C \times SU(3)_L$ gauge symmetry, in a similar way as done in the 331 model with D_4 flavor symmetry of Ref. [150]. Those charged vector like leptons should have the appropriate transformation properties under the discrete groups of our model in such a way to allow them having Yukawa interactions with the SM charged leptons. This will give rise to one loop level contributions to the muon anomalous magnetic moment mediated by charged vector like leptons and neutral scalars running in the internal lines of the loop. Under these conditions the muon $g-2$ anomaly can be successfully accommodated for an appropriate region of parameter space provided that such exotic charged vector like leptons are included in the fermionic spectrum of our model. We do not perform such fermionic extension in this work since recent lattice QCD calculations of the hadronic vacuum polarization (HVP) contribution of the muon magnetic moment [151–154] lead to a 1.5σ deviation [155] of its SM prediction from the

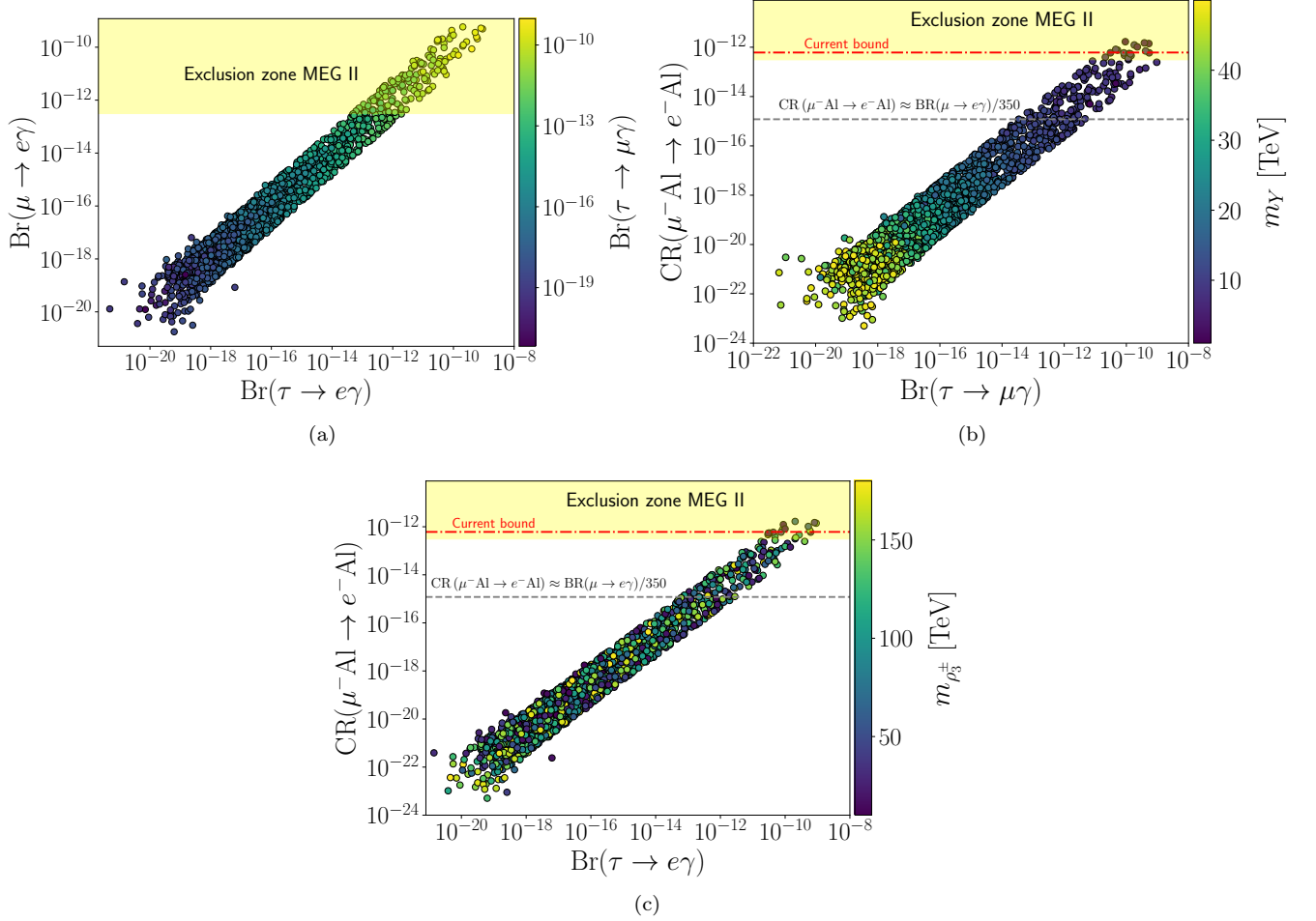


Figure 8: Correlation between the branching ratios $\text{Br}(\mu \rightarrow e\gamma)$ and $\text{Br}(\tau \rightarrow e\gamma)$ (panel (a)), $\text{Br}(\tau \rightarrow \mu\gamma)$ and the conversion rate $\text{CR}(\mu^- \text{Al} \rightarrow e^- \text{Al})$ (panel (b)) and $\text{Br}(\tau \rightarrow e\gamma)$ and the conversion rate $\text{CR}(\mu^- \text{Al} \rightarrow e^- \text{Al})$. The color gradient represents the values of $\text{Br}(\tau \rightarrow \mu\gamma)$ in panel (a), the gauge boson mass m_γ in panel (b) and the charged scalar mass $m_{\rho_3^\pm}$ in panel (c). The yellow shaded region corresponds to the exclusion zone from the MEG II experiment [142], the red dot dashed line indicates the current bound for $\mu \rightarrow e$ conversion in titanium (Ti) nuclei [149] and the gray dashed line represents the boundary approximated by Eq. (73).

corresponding experimental value and in addition, a recent study of the hadronic vacuum polarization contribution to the muon $g - 2$ at long distances has found that the SM prediction for the total muon anomalous magnetic moment is in agreement with the current experimental average [156].

Although the model includes sources of CP violation through complex Yukawa couplings and active–sterile neutrino mixing, the contributions to the electron electric dipole moment (EDM) are strongly suppressed. This suppression is due to the large masses of the new charged scalar ρ_3^\pm and the exotic gauge boson Y^\pm , which, due to flavour constraints, are typically required to lie above the multi-TeV scale. As pointed out in Ref. [157], the corresponding Wilson coefficients scale inversely with the square of these masses. Furthermore, the structure imposed by the $A_4 \times Z_N$ flavour symmetries tends to align the Yukawa couplings and reduce the number of physical CP-violating phases. Together with the small active–sterile mixing parameters resulting from the bounds imposed by charged lepton flavour-violating processes, it follows that the predicted contributions to the electric dipole moment d_e of the electron are well below the current experimental sensitivity. Therefore, the electron EDM does not place any significant constraint on the model parameter space.

To conclude this section, we present some remarks on the decays of quasi-Dirac sterile neutrinos and compare our predictions for these decays and lepton flavor violating (LFV) signals with those obtained in other models featuring extended gauge symmetries. Similar to the $U'(1)$ model discussed in Ref. [158], our model predicts that sterile neutrinos undergo two-body decays: $N \rightarrow l_i^\pm W^\mp$, $\nu_i Z$ and $\nu_i h$ (where $i = 1, 2, 3$ is a flavor index). These decay

m_{n_4}	m_{n_5}	m_{n_6}	m_{n_7}	m_{n_8}	m_{n_9}	m_Y	$m_{\rho_3^\pm}$	$\text{Br}(\mu \rightarrow e\gamma)$	$\text{Br}(\tau \rightarrow e\gamma)$	$\text{Br}(\tau \rightarrow \mu\gamma)$	$\text{CR}(\mu\text{Al} \rightarrow e\text{Al})$
4.90	3.52	2.81	3.98	3.23	5.57	10.21	118.99	7.14×10^{-13}	1.79×10^{-13}	1.23×10^{-12}	2.04×10^{-15}
5.37	0.95	1.79	3.23	4.63	1.43	12.84	65.78	1.41×10^{-13}	1.16×10^{-13}	2.16×10^{-14}	4.03×10^{-16}
3.35	2.55	3.07	2.95	1.65	5.82	13.28	167.09	1.65×10^{-13}	3.57×10^{-14}	6.21×10^{-14}	4.72×10^{-16}
2.14	4.31	2.74	5.83	4.47	5.48	10.56	173.46	3.16×10^{-14}	1.96×10^{-13}	3.12×10^{-13}	9.04×10^{-17}
1.47	2.34	1.64	4.60	1.78	4.42	11.22	150.23	2.59×10^{-14}	4.71×10^{-14}	1.61×10^{-13}	7.41×10^{-17}
1.01	5.78	4.70	4.29	1.95	5.84	17.61	118.51	9.32×10^{-15}	7.66×10^{-15}	1.44×10^{-15}	2.66×10^{-17}
4.71	3.30	2.58	3.73	1.70	3.47	14.00	177.13	7.98×10^{-15}	2.41×10^{-14}	2.17×10^{-14}	2.28×10^{-17}
2.94	3.44	1.41	4.70	4.79	5.47	15.59	39.34	3.17×10^{-16}	4.58×10^{-16}	1.95×10^{-16}	9.05×10^{-19}
2.40	1.45	5.88	5.92	4.47	2.16	18.42	28.29	6.02×10^{-16}	8.22×10^{-16}	3.11×10^{-15}	1.72×10^{-18}
4.33	4.22	4.41	4.93	2.57	3.17	25.87	63.28	1.86×10^{-17}	7.04×10^{-17}	7.33×10^{-17}	5.30×10^{-20}
1.21	2.22	1.32	4.38	1.35	3.98	23.03	42.50	1.98×10^{-17}	5.38×10^{-17}	1.46×10^{-16}	5.65×10^{-20}
3.19	1.92	1.15	3.89	3.59	1.22	37.17	126.11	5.27×10^{-18}	3.43×10^{-18}	5.48×10^{-19}	1.51×10^{-20}
2.43	2.85	5.25	0.95	3.76	3.65	45.50	34.87	3.27×10^{-18}	1.97×10^{-18}	5.58×10^{-19}	9.36×10^{-21}
4.75	2.02	1.03	4.09	4.58	4.68	45.53	55.09	3.63×10^{-19}	6.12×10^{-19}	3.25×10^{-19}	1.04×10^{-21}
3.99	1.85	3.44	3.75	5.96	4.04	40.51	102.52	3.30×10^{-19}	1.87×10^{-19}	9.21×10^{-19}	9.41×10^{-22}

Table V: Branching ratios for the LFV decays. The first to sixth columns present the numerical values of the heavy neutrino masses m_{n_i} in TeV. The seventh and eighth columns show the mass of the gauge boson m_Y and the charged scalar mass $m_{\rho_3^\pm}$ in TeV, respectively. The subsequent columns display the branching ratios for the processes $\mu \rightarrow e\gamma$, $\tau \rightarrow e\gamma$, and $\tau \rightarrow \mu\gamma$, respectively. The final column shows the estimated conversion for the process $\mu\text{Al} \rightarrow e\text{Al}$.

modes are suppressed due to the small active-sterile neutrino mixing angle, $\theta \sim \mathcal{O}(10^{-2})$. The above mentioned two body decays lead to three-body decays: $N \rightarrow l_i^+ l_j^- \nu_k$, $N \rightarrow l_i^- u_j d_k$, $N \rightarrow b\bar{b}\nu_k$ (where $i, j, k = 1, 2, 3$ are flavor indices), which are also present in the $U'(1)$ model of Ref. [158]. As a result, we anticipate similar predictions for the total cross section of the LFV process $pp \rightarrow NN \rightarrow e^\pm \mu^\mp 4j$, as well as for sterile neutrino decays, compared to those found in Ref. [158]. However, a slight deviation is expected in the decay rate of $N \rightarrow l_i^+ l_j^- \nu_k$, as our model includes contributions from off-shell W and W' gauge bosons whereas in Ref. [158], only the off-shell W boson contributes. Notably, the contribution from the off-shell W' boson in our model is significantly suppressed by a factor of approximately $\frac{M_W^4}{M_{W'}^4}$ relative to the contribution from the W boson. Furthermore, we anticipate similar predictions for sterile neutrino decay rates and the cross section of the LFV process $pp \rightarrow NN \rightarrow e^\pm \mu^\mp$ to those found in the left-right symmetric model of Refs. [126, 127]. However, the charged lepton flavor violating process $\mu \rightarrow e\gamma$ serves as a key discriminator between our model and the left-right symmetric model of Refs. [126, 127]. In our case, the dominant contributions to $\mu \rightarrow e\gamma$ originates from loop diagrams involving W' and charged scalar exchanges, whereas in the left-right symmetric models of Refs. [126, 127], such CLFV process receives contributions from the virtual exchange of the W_R gauge boson and the doubly charged scalars running in the internal lines of the loop.

VIII. CONCLUSIONS

We have constructed a $SU(3)_C \times SU(3)_L \times U(1)_X$ model based on the A_4 flavor symmetry. This version is different from previous versions by incorporating the $U(1)_{L_g}$ global lepton number symmetry and the $Z_2 \times Z'_2 \times Z_3 \times Z_4 \times Z_7 \times Z_{10}$ discrete group. The model introduces right-handed neutrinos as the third components of the $SU(3)_L$ leptonic triplets and three additional neutral fermions, N_{aR} to generate the light neutrino masses through an inverse seesaw mechanism. The smallness of the μ parameter of the inverse seesaw is attributed to higher-dimensional Yukawa operators which give rise small lepton number violating Majorana mass terms parameters after the spontaneous breaking of the $U(1)_{L_g}$ global symmetry.

The A_4, Z_3, Z_4 and Z_7 symmetries ensure that the top quark is generated from a renormalizable Yukawa interaction, whereas the masses of lighter fermions arise from non-renormalizable Yukawa interactions after the spontaneous breaking of discrete symmetries. In addition, these discrete symmetries allow for a reduction of fermion sector parameters and yield a hierarchical structure in the entries of the SM charged fermion mass matrices, which effectively explains the SM charged fermion masses and quark mixing pattern. Due to the discrete symmetries of the model,

the quark mixing arises only from the up-type quark sector. The Z_{10} symmetry distinguishes the A_4 scalar triplets participating in the quark and neutrino Yukawa interactions from the ones appearing in the charged lepton Yukawa terms, then allowing us to separate the mixing in the neutrino and quark sectors. The model successfully predicts SM fermion masses and mixing patterns, consistent with experimental observations. The sizable neutrino Yukawa couplings predicted by the model could lead to observable rates of cLFV processes, which could be tested in future experiments.

ACKNOWLEDGMENTS

The authors are very grateful to L.T. Hue, for his involvement in the initial stages of the project and for very useful discussions. This research has received funding from Fondecyt (Chile), Grants No. 1210378, No. 1241855, No 1210131, ANID PIA/APOYO AFB230003 and Proyecto Milenio-ANID: ICN2019_044. D.T.Huong acknowledges the financial support of the Vietnam Academy of Science and Technology under Grant No. NVCC05.05/24-25.

Appendix A: The product rules for A_4

The A_4 group has one three-dimensional $\mathbf{3}$ and three distinct one-dimensional $\mathbf{1}$, $\mathbf{1}'$ and $\mathbf{1}''$ irreducible representations, satisfying the following product rules:

$$\mathbf{3} \otimes \mathbf{3} = \mathbf{3}_s \oplus \mathbf{3}_a \oplus \mathbf{1} \oplus \mathbf{1}' \oplus \mathbf{1}'', \quad (\text{A1})$$

$$\mathbf{1} \otimes \mathbf{1} = \mathbf{1}, \quad \mathbf{1}' \otimes \mathbf{1}'' = \mathbf{1}, \quad \mathbf{1}' \otimes \mathbf{1}' = \mathbf{1}'', \quad \mathbf{1}'' \otimes \mathbf{1}'' = \mathbf{1}',$$

Considering (x_1, x_2, x_3) and (y_1, y_2, y_3) as the basis vectors for two A_4 -triplets $\mathbf{3}$, the following relations are fulfilled:

$$\begin{aligned} (\mathbf{3} \otimes \mathbf{3})_{\mathbf{1}} &= x_1 y_1 + x_2 y_2 + x_3 y_3, & (\text{A2}) \\ (\mathbf{3} \otimes \mathbf{3})_{\mathbf{3}_s} &= (x_2 y_3 + x_3 y_2, x_3 y_1 + x_1 y_3, x_1 y_2 + x_2 y_1), & (\mathbf{3} \otimes \mathbf{3})_{\mathbf{1}'} &= x_1 y_1 + \omega x_2 y_2 + \omega^2 x_3 y_3, \\ (\mathbf{3} \otimes \mathbf{3})_{\mathbf{3}_a} &= (x_2 y_3 - x_3 y_2, x_3 y_1 - x_1 y_3, x_1 y_2 - x_2 y_1), & (\mathbf{3} \otimes \mathbf{3})_{\mathbf{1}''} &= x_1 y_1 + \omega^2 x_2 y_2 + \omega x_3 y_3, \end{aligned}$$

where $\omega = e^{i\frac{2\pi}{3}}$. The representation $\mathbf{1}$ is trivial, while the non-trivial $\mathbf{1}'$ and $\mathbf{1}''$ are complex conjugate to each other. Some reviews of discrete symmetries in particle physics are found in Refs. [159–162].

Appendix B: Higgs sector

The renormalized Higgs potential respecting the whole symmetry group mentioned in this work is:

$$\begin{aligned} V_H &= V_{H,2} + V_{H,3} + V_{H,4}, \\ V_{H,2} &= \sum_{k=1}^{13} \bar{\mu}_{s_k}^2 \left(s_k^\dagger s_k \right)_1 + \left(\mu_{1\zeta\vartheta}^2 \zeta\vartheta^* + \mu_\zeta^2 \zeta^2 + \mu_{\zeta\vartheta}^2 \zeta\vartheta + \mu_\eta^2 \eta^2 + \mu_{\Phi\Xi}^2 \Xi^* \Phi + \mu_\vartheta^2 \vartheta^2 + \text{H.c.} \right)_1, \\ V_{H,3} &= \eta \left(\eta^2 \lambda_\eta + \lambda_\eta^{(1)} \eta \eta^* + \lambda_{\eta\zeta} \zeta^2 + \lambda_{\eta\zeta}^{(1)} \zeta \zeta^* + \lambda_{\eta\zeta}^{(2)} \zeta^{*2} + \lambda_{\eta\zeta\vartheta} \zeta\vartheta + \lambda_{\eta\zeta\vartheta}^{(1)} \zeta\vartheta^* + \lambda_{\eta\zeta\vartheta}^{(2)} \zeta^* \vartheta \right. \\ &\quad \left. + \lambda_{\eta\zeta\vartheta}^{(3)} \zeta^* \vartheta^* + \lambda_{\eta\xi} \xi \xi^* + \lambda_{\eta\Xi} \Xi \Xi^* + \lambda_{\eta\Phi} \Phi^* \Phi + \lambda_{\eta\Phi\Xi} \Xi^* \Phi + \lambda_{\eta\Phi\Xi}^{(1)} \Xi \Phi^* \right. \\ &\quad \left. + \lambda_{\eta\vartheta} \vartheta^2 + \lambda_{\eta\vartheta}^{(1)} \vartheta^* \vartheta + \lambda_{\eta\phi} \phi^* \phi \right) + \lambda_{\eta\xi\varphi} (\eta\xi)_{1'} \varphi^* + \lambda_{\eta\xi\varphi}^{(1)} (\eta\xi^*)_{1''} \varphi + \text{H.c.}, \\ V_{H,4} &= \sum_{k=1}^{13} \bar{\lambda}_{s_k} \left(s_k^\dagger s_k \right)^2 + \sum_{k,l=1,l<k}^{13} \bar{\lambda}_{s_k s_l} \left(s_k^\dagger s_k \right) \left(s_l^\dagger s_l \right) + \bar{\lambda}_{2\chi\rho} \left(\chi^\dagger \rho \right) \left(\rho^\dagger \chi \right) \\ &\quad + \sum_{k=1,2} \left[\left(s_k^\dagger s_k \right) \left(\lambda_{s_k \zeta} \zeta^2 + \lambda_{s_k \zeta\vartheta} \zeta\vartheta + \lambda_{s_k \zeta\vartheta}^{(1)} \zeta\vartheta^* + \lambda_{s_k \eta} \eta^2 + \lambda_{s_k \Phi\Xi} \Xi^* \Phi + \lambda_{s_k \vartheta} \vartheta^2 \right)_1 + \text{H.c.} \right], \\ &\quad + V_{H,4}^{(1)} + V_{H,4}^{(2)}, \end{aligned}$$

$$\begin{aligned}
V_{H,4}^{(1)} = & \zeta^4 \lambda_\zeta + \zeta^3 \left(\lambda_\zeta^{(1)} \zeta^* + \lambda_{\zeta\vartheta} \vartheta + \lambda_{\zeta\vartheta}^{(1)} \vartheta^* \right) + \zeta \left(\lambda_{\zeta\vartheta}^{(10)} \vartheta^{*2} + \lambda_{\zeta\vartheta}^{(11)} \vartheta^{*3} + \lambda_{\zeta\vartheta}^{(7)} \vartheta^3 + \lambda_{\zeta\vartheta}^{(8)} \zeta^* \vartheta^2 + \lambda_{\zeta\vartheta}^{(9)} \vartheta^* \vartheta^2 \right) \\
& + \zeta^2 \left[\lambda_{\zeta\vartheta}^{(2)} \vartheta^2 + \zeta^* \left(\lambda_{\zeta\vartheta}^{(3)} \vartheta + \lambda_{\zeta\vartheta}^{(5)} \vartheta^* \right) + \lambda_{\zeta\vartheta}^{(4)} \vartheta^* \vartheta + \lambda_{\zeta\vartheta}^{(6)} \vartheta^{*2} \right] + \lambda_{\vartheta} \vartheta^4 + \lambda_{\vartheta}^{(1)} \vartheta^* \vartheta^3 \\
& + \lambda_{\zeta\vartheta\Phi\Xi} \zeta \Xi^* \Phi \vartheta + \lambda_{\zeta\vartheta\Phi\Xi}^{(1)} \zeta \Xi \Phi^* \vartheta + \lambda_{\zeta\vartheta\Phi\Xi}^{(2)} \zeta \Xi^* \vartheta^* \Phi + \lambda_{\zeta\vartheta\Phi\Xi}^{(3)} \zeta \Xi \Phi^* \vartheta^* \\
& + \phi \left(\lambda_{\zeta\phi\Phi\Xi} \zeta \Xi \Phi + \lambda_{\vartheta\phi\Phi\Xi} \Xi \Phi \vartheta + \lambda_{\phi\Xi}^{(1)} \Xi^{*3} + \lambda_{\phi\Phi}^{(1)} \Phi^{*3} \right) \\
& + \phi^* \left(\lambda_{\zeta\phi\Phi\Xi}^{(1)} \zeta \Xi^* \Phi^* + \lambda_{\vartheta\phi\Phi\Xi}^{(1)} \Xi^* \Phi^* \vartheta \right) + \lambda_\eta \eta^4 + \lambda_\eta^{(1)} \eta^3 \eta^* + \phi^3 (\lambda_{\phi\Xi} \Xi + \lambda_{\phi\Phi} \Phi) \\
& + \xi \xi^* \left(\lambda_{\zeta\xi} \zeta^2 + \lambda_{\zeta\vartheta\xi} \zeta \vartheta + \lambda_{\zeta\vartheta\xi}^{(1)} \zeta \vartheta^* + \lambda_{\Phi\Xi\xi} \Xi^* \Phi + \lambda_{\vartheta\xi} \vartheta^2 \right) \\
& + \eta^2 \left(\lambda_{\eta\zeta} \zeta^2 + \lambda_{\eta\zeta}^{(1)} \zeta \zeta^* + \lambda_{\eta\zeta}^{(2)} \zeta^{*2} + \lambda_{\eta\zeta\vartheta} \zeta \vartheta + \lambda_{\eta\zeta\vartheta}^{(1)} \zeta \vartheta^* + \lambda_{\eta\zeta\vartheta}^{(2)} \zeta^* \vartheta + \lambda_{\eta\zeta\vartheta}^{(3)} \zeta^* \vartheta^* + \lambda_{\eta\xi} \xi^* \xi \right. \\
& \quad \left. + \lambda_{\eta\Xi} \Xi \Xi^* + \lambda_{\eta\Phi} \Phi^* \Phi + \lambda_{\eta\Phi\Xi} \Xi^* \Phi + \lambda_{\eta\Phi\Xi}^{(1)} \Xi \Phi^* + \lambda_{\eta\vartheta} \vartheta^2 + \lambda_{\eta\vartheta}^{(1)} \vartheta^* \vartheta + \lambda_{\eta\vartheta}^{(2)} \vartheta^{*2} + \lambda_{\eta\phi} \phi^* \phi \right) \\
& + \eta \eta^* \left(\lambda_{\eta\zeta}^{(3)} \zeta^2 + \lambda_{\eta\zeta\vartheta}^{(4)} \zeta \vartheta + \lambda_{\eta\zeta\vartheta}^{(5)} \zeta \vartheta^* + \lambda_{\eta\Phi\Xi}^{(2)} \Xi^* \Phi + \lambda_{\eta\vartheta}^{(3)} \vartheta^2 \right) \\
& + \zeta^2 \left(\lambda_{\zeta\Xi} \Xi \Xi^* + \lambda_{\zeta\Phi} \Phi^* \Phi + \lambda_{\zeta\Phi\Xi} \Xi^* \Phi + \lambda_{\zeta\Phi\Xi}^{(1)} \Xi \Phi^* \right) \\
& + \zeta \left[\lambda_{\zeta\Phi\Xi}^{(2)} \zeta^* \Xi^* \Phi + \vartheta (\lambda_{\zeta\vartheta\Xi} \Xi \Xi^* + \lambda_{\zeta\vartheta\Phi} \Phi^* \Phi) + \vartheta^* \left(\lambda_{\zeta\vartheta\Xi}^{(1)} \Xi \Xi^* + \lambda_{\zeta\vartheta\Phi}^{(1)} \Phi^* \Phi \right) \right] \\
& + \phi \phi^* \left[\left(\lambda_{\zeta\vartheta\phi} \vartheta + \lambda_{\zeta\vartheta\phi}^{(1)} \vartheta^* \right) \zeta + \lambda_{\zeta\phi} \zeta^2 + \lambda_{\vartheta\phi} \vartheta^2 + \lambda_{\phi\Phi\Xi} \Xi^* \Phi \right] \\
& + \phi^2 \left[\zeta (\lambda_{\zeta\Phi\Xi} \Xi^* + \lambda_{\zeta\phi\Phi} \Phi^*) + \vartheta (\lambda_{\vartheta\Phi\Xi} \Xi^* + \lambda_{\vartheta\phi\Phi} \Phi^*) \right] + \phi^{*2} \left[\zeta \left(\lambda_{\zeta\Phi\Xi}^{(2)} \Xi + \lambda_{\zeta\phi\Phi}^{(2)} \Phi \right) + \vartheta \left(\lambda_{\vartheta\Phi\Xi}^{(2)} \Xi + \lambda_{\vartheta\phi\Phi}^{(2)} \Phi \right) \right] \\
& + \phi \left[\zeta \left(\lambda_{\zeta\Phi\Xi}^{(1)} \Xi^2 + \lambda_{\zeta\phi\Phi}^{(1)} \Phi^2 \right) + \vartheta \left(\lambda_{\vartheta\Phi\Xi}^{(1)} \Xi^2 + \lambda_{\vartheta\phi\Phi}^{(1)} \Phi^2 \right) + \lambda_{\phi\Phi\Xi}^{(1)} \Xi^* \Phi^{*2} + \lambda_{\phi\Phi\Xi}^{(2)} \Xi^{*2} \Phi^* \right] \\
& + \phi^* \left[\zeta \left(\lambda_{\zeta\Phi\Xi}^{(3)} \Xi^{*2} + \lambda_{\zeta\phi\Phi}^{(3)} \Phi^{*2} \right) + \vartheta \left(\lambda_{\vartheta\Phi\Xi}^{(3)} \Xi^{*2} + \lambda_{\vartheta\phi\Phi}^{(3)} \Phi^{*2} \right) \right] + \lambda_{\Phi\Xi} \Xi^* \Phi^* \Phi^2 + \lambda_{\Phi\Xi}^{(1)} \Xi^{*2} \Phi^2 + \lambda_{\Phi\Xi}^{(2)} \Xi \Xi^{*2} \Phi \\
& + \vartheta^2 \left(\lambda_{\vartheta\Xi} \Xi \Xi^* + \lambda_{\vartheta\Phi} \Phi^* \Phi + \lambda_{\vartheta\Phi\Xi} \Xi^* \Phi + \lambda_{\vartheta\Phi\Xi}^{(1)} \Xi \Phi^* \right) + \lambda_{\vartheta\Phi\Xi}^{(2)} \Xi^* \Phi \vartheta^* \vartheta + \text{H.c.}, \\
V_{H,4}^{(2)} = & \sum_{k=3}^5 s_k s_k^* \left(\lambda_{s_k \zeta} \zeta^2 + \lambda_{s_k \zeta \vartheta} \zeta \vartheta + \lambda_{s_k \zeta \vartheta}^{(1)} \zeta \vartheta^* + \lambda_{s_k \eta} \eta^2 + \lambda_{s_k \Phi\Xi} \Xi^* \Phi + \lambda_{s_k \vartheta} \vartheta^2 \right)_1 \\
& + \varphi \varphi^* \left(\lambda_{\zeta\varphi} \zeta^2 + \lambda_{\zeta\vartheta\varphi} \zeta \vartheta + \lambda_{\zeta\vartheta\varphi}^{(1)} \zeta \vartheta^* + \lambda_{\eta\varphi} \eta^2 + \lambda_{\Phi\Xi\varphi} \Xi^* \Phi + \lambda_{\vartheta\varphi} \vartheta^2 \right)_1 + \lambda_{\xi\varphi}^{(1)} (\xi^2)_{1''} \varphi^{*2} \\
& + \varphi^* \xi \left(\lambda_{\zeta\xi\varphi} \zeta^2 + \lambda_{\zeta\xi\varphi}^{(2)} \zeta \zeta^* + \lambda_{\zeta\vartheta\xi\varphi} \zeta \vartheta + \lambda_{\zeta\vartheta\xi\varphi}^{(2)} \zeta \vartheta^* + \lambda_{\eta\xi\varphi} \eta^2 + \lambda_{\eta\xi\varphi}^{(2)} \eta \eta^* + \lambda_{\Xi\xi\varphi} \Xi \Xi^* + \lambda_{\Phi\Xi\xi\varphi} \Xi^* \Phi \right) \\
& + \lambda_{\Phi\xi\varphi} \Phi^* \Phi + \lambda_{\vartheta\xi\varphi} \vartheta^2 + \lambda_{\vartheta\xi\varphi}^{(2)} \vartheta^* \vartheta + \lambda_{\phi\xi\varphi} \phi^* \phi \Big) + \lambda_{\xi\varphi} \varphi^* \xi^2 \xi^* \\
& + \varphi \xi^* \left(\lambda_{\zeta\xi\varphi}^{(1)} \zeta^2 + \lambda_{\zeta\vartheta\xi\varphi}^{(1)} \zeta \vartheta + \lambda_{\zeta\vartheta\xi\varphi}^{(3)} \zeta \vartheta^* + \lambda_{\eta\xi\varphi}^{(1)} \eta^2 + \lambda_{\Phi\Xi\xi\varphi} \Xi^* \Phi + \lambda_{\vartheta\xi\varphi}^{(1)} \vartheta^2 \right) + \text{H.c.}, \tag{B1}
\end{aligned}$$

where s_k runs over A_4 Higgs representations introduced in this model, $s_k = \chi, \rho, \sigma_1, \sigma_2, \sigma_3, \eta, \zeta, \vartheta, \phi, \Phi, \Xi, \xi, \varphi$ corresponding to the orders appearing in Table I: $k = 1, 2, 3, \dots, 13$. The $SU(3)_L$ Higgs triplets χ and ρ only appear in $V_{H,2}$ and the two first lines of $V_{H,4}$. In contrast, $V_{H,3}$, $V_{H,4}^{(1)}$, and $V_{H,4}^{(2)}$ consist of only $SU(3)_L$ singlets. Except two terms with A_4 singlets φ and φ^* , all terms in $V_{H,3}$ are products of three A_4 triplets. The Lagrangian part $V_{H,4}^{(1)}$ consists of all products of four A_4 triplets. The first and second lines of $V_{H,4}^{(2)}$ consist of products of two A_4 singlets with two A_4 triplets. The remaining lines consist of products of one A_4 singlet with three A_4 triplets

The expansion rule for determining invariant terms of a product of three A_4 triplets $s_i s_j s_k$ is

$$\lambda_x s_i s_j s_k \equiv \lambda_{x,1} \left[(s_i s_j)_{3_s} s_k \right]_1 + \lambda_{x,2} \left[(s_i s_j)_{3_a} s_k \right]_1, \tag{B2}$$

where λ_x , $\lambda_{x,1}$, and $\lambda_{x,2}$ are couplings, implying that every term having three A_4 triplets in $V_{H,3}$ and $V_{H,4}^{(2)}$ stands for two independent terms, in general. Note that $(s_i s_i)_{3_a} = 0$, hence the first term automatically vanish if $i = j$.

The expansions of products of the four reps. 3 of the A_4 symmetry for every term $\lambda s_i s_j s_k s_l$ in $V_{H,4}^{(1)}$ are defined generally as:

$$[\lambda (s_i s_j) (s_k s_l)]_1 \equiv \lambda_1 (s_i s_j)_1 (s_k s_l)_1 + \lambda_2 (s_i s_j)_{1'} (s_k s_l)_{1''} + \lambda_3 (s_i s_j)_{1''} (s_k s_l)_{1'} + \lambda_4 [(s_i s_j)_{3_s} (s_k s_l)_{3_s}]_1$$

$$+ \lambda_5 [(s_i s_j)_{3s} (s_k s_l)_{3a}]_1 + \lambda_6 [(s_i s_j)_{3a} (s_k s_l)_{3s}]_1 + \lambda_7 [(s_i s_j)_{3a} (s_k s_l)_{3a}]_1, \quad (\text{B3})$$

where λ is the coupling appearing in the Higgs potential (B1), while λ_i with $i = 1, 2, 3, \dots, 7$ are the independent couplings corresponding to the seven A_4 invariant terms. For the Higgs sector introduced in this work, the products like $[(s_i s_k)(s_j s_l)]_1, [(s_i s_l)(s_j s_k)]_1, \dots$ are not included in the Higgs potential because we can prove that they are always written in terms of linear combinations of the seven A_4 products given in Eq. B3.

Let us note that due to the antisymmetry and symmetry properties of the $\mathbf{3}_a$ and $\mathbf{3}_s$ triplet components in the products $(s_i s_j)$, we obtain $(\mathbf{3}_s \mathbf{3}_a)_1 + \text{H.c.} = 0$. Hence many terms having this invariance does not appear in the Higgs potential.

With the Higgs potential given above, the VEV patterns satisfy the all the equations corresponding to the minimal conditions of the Higgs potential.

The masses and mixing parameters of the singly charged Higgs boson are computed in the general cases of the Higgs potential, the minimal equation automatically satisfies $\frac{\partial V_H}{\partial \chi_1^0} = 0$ at $\chi_1^0 = \langle \chi_1^0 \rangle = 0$. Using two other equations $\frac{\partial V_H}{\partial \chi_3} = 0$ and $\frac{\partial V_H}{\partial \rho_2} = 0$ at the corresponding VEVs, we write $\bar{\mu}_\chi^2$ and $\bar{\mu}_\rho^2$ as the functions of other parameters in the Higgs potential as follows:

$$\begin{aligned} \bar{\mu}_\chi^2 &= c_\gamma^2 (-2c_a^2 v_\zeta^2 \lambda \chi \zeta - \bar{\lambda}_{\chi\zeta} v_\zeta^2 - \bar{\lambda}_{\chi\Xi} v_\Xi^2) - c_\gamma s_\alpha s_\gamma v_\zeta v_\vartheta \lambda \chi \zeta \vartheta - \frac{\bar{\lambda}_{1\chi\rho} v_\rho^2}{2} - \bar{\lambda}_\chi v_\chi^2 + v_\eta^2 (-\bar{\lambda}_{\chi\eta} - 2\lambda\chi\eta) - \bar{\lambda}_{\chi\xi} v_\xi^2 \\ &\quad - \frac{\bar{\lambda}_{\chi\sigma 1} v_{\sigma 1}^2}{2} - \frac{\bar{\lambda}_{\chi\sigma 2} v_{\sigma 2}^2}{2} - \frac{\bar{\lambda}_{\chi\sigma 3} v_{\sigma 3}^2}{2} - \frac{\bar{\lambda}_{\chi\varphi} v_\varphi^2}{3} + s_\gamma^2 (-\bar{\lambda}_{\chi\Phi} v_\Phi^2 - \bar{\lambda}_{\chi\vartheta} v_\vartheta^2) - \bar{\lambda}_{\chi\phi} v_\phi^2, \\ \bar{\mu}_\rho^2 &= c_\gamma^2 (-2c_a^2 v_\zeta^2 \lambda \rho \zeta - \bar{\lambda}_{\rho\zeta} v_\zeta^2 - \bar{\lambda}_{\rho\Xi} v_\Xi^2) - c_\gamma s_\alpha s_\gamma v_\zeta v_\vartheta \lambda \rho \zeta \vartheta - \frac{\bar{\lambda}_{1\rho\chi} v_\chi^2}{2} - \bar{\lambda}_\rho v_\rho^2 + v_\eta^2 (-\bar{\lambda}_{\rho\eta} - 2\lambda\rho\eta) - \bar{\lambda}_{\rho\xi} v_\xi^2 \\ &\quad - \frac{\bar{\lambda}_{\rho\sigma 1} v_{\sigma 1}^2}{2} - \frac{\bar{\lambda}_{\rho\sigma 2} v_{\sigma 2}^2}{2} - \frac{\bar{\lambda}_{\rho\sigma 3} v_{\sigma 3}^2}{2} - \frac{\bar{\lambda}_{\rho\varphi} v_\varphi^2}{3} + s_\gamma^2 (-\bar{\lambda}_{\rho\Phi} v_\Phi^2 - \bar{\lambda}_{\rho\vartheta} v_\vartheta^2) - \bar{\lambda}_{\rho\phi} v_\phi^2. \end{aligned} \quad (\text{B4})$$

Inserting these into the Higgs potential, we easily find that ρ_1^\pm are exactly the Goldstone bosons absorbed by the SM charged gauge bosons W^\pm . On the other hand the two components χ_2^- and ρ_3^- mix with each other to result in a Goldstone boson G_Y^- of the heavy charged gauge boson Y^- and a physical charged Higgs boson h^- . The mixing and masses are

$$\begin{pmatrix} \chi_2^\pm \\ \rho_3^\pm \end{pmatrix} = C_\pm \begin{pmatrix} G_Y^\pm \\ h^\pm \end{pmatrix}, \quad C_\pm = \begin{pmatrix} c_x & s_x \\ -s_x & c_x \end{pmatrix}, \quad m_{h^\pm}^2 = \frac{\bar{\lambda}_{2\chi\rho}}{2} (v_\rho^2 + v_\chi^2), \quad (\text{B5})$$

where $c_x \equiv \cos \theta_x$, $s_x \equiv \sin \theta_x$, and

$$t_x \equiv \tan \theta_x = \frac{v_\rho}{v_\chi}. \quad (\text{B6})$$

-
- [1] A. B. McDonald, ‘‘Nobel Lecture: The Sudbury Neutrino Observatory: Observation of flavor change for solar neutrinos,’’ *Rev.Mod.Phys.* **88** (2016) 030502.
- [2] T. Kajita, ‘‘Nobel Lecture: Discovery of atmospheric neutrino oscillations,’’ *Rev.Mod.Phys.* **88** (2016) 030501.
- [3] P. de Salas *et al.*, ‘‘2020 global reassessment of the neutrino oscillation picture,’’ *JHEP* **02** (2021) 071, [arXiv:2006.11237 \[hep-ph\]](https://arxiv.org/abs/2006.11237).
- [4] **Planck** Collaboration, N. Aghanim *et al.*, ‘‘Planck 2018 results. VI. Cosmological parameters,’’ *Astron. Astrophys.* **641** (2020) A6, [arXiv:1807.06209 \[astro-ph.CO\]](https://arxiv.org/abs/1807.06209). [Erratum: *Astron.Astrophys.* 652, C4 (2021)].
- [5] N. Cabibbo, ‘‘Unitary symmetry and leptonic decays,’’ *Phys. Rev. Lett.* **10** (Jun, 1963) 531–533. <https://link.aps.org/doi/10.1103/PhysRevLett.10.531>.
- [6] M. Kobayashi and T. Maskawa, ‘‘CP Violation in the Renormalizable Theory of Weak Interaction,’’ *Prog. Theor. Phys.* **49** (1973) 652–657.
- [7] Z. Maki, M. Nakagawa, and S. Sakata, ‘‘Remarks on the unified model of elementary particles,’’ *Prog. Theor. Phys.* **28** (1962) 870–880.
- [8] S. T. Petcov, ‘‘The Processes $\mu \rightarrow e + \gamma, \mu \rightarrow e + \bar{e}, \nu' \rightarrow \nu + \gamma$ in the Weinberg-Salam Model with Neutrino Mixing,’’ *Sov. J. Nucl. Phys.* **25** (1977) 340. [Erratum: *Sov.J.Nucl.Phys.* 25, 698 (1977), Erratum: *Yad.Fiz.* 25, 1336 (1977)].
- [9] W. J. Marciano and A. I. Sanda, ‘‘Exotic Decays of the Muon and Heavy Leptons in Gauge Theories,’’ *Phys. Lett. B* **67** (1977) 303–305.

- [10] B. W. Lee, S. Pakvasa, R. E. Shrock, and H. Sugawara, “Muon and electron number nonconservation in a $v - a$ gauge model,” *Phys. Rev. Lett.* **38** (Apr, 1977) 937–939. <https://link.aps.org/doi/10.1103/PhysRevLett.38.937>.
- [11] B. W. Lee and R. E. Shrock, “Natural suppression of symmetry violation in gauge theories: Muon- and electron-lepton-number nonconservation,” *Phys. Rev. D* **16** (Sep, 1977) 1444–1473. <https://link.aps.org/doi/10.1103/PhysRevD.16.1444>.
- [12] E. Ma and G. Rajasekaran, “Softly broken $A(4)$ symmetry for nearly degenerate neutrino masses,” *Phys. Rev.* **D64** (2001) 113012, [arXiv:hep-ph/0106291](https://arxiv.org/abs/hep-ph/0106291) [hep-ph].
- [13] X.-G. He, Y.-Y. Keum, and R. R. Volkas, “ $A(4)$ flavor symmetry breaking scheme for understanding quark and neutrino mixing angles,” *JHEP* **04** (2006) 039, [arXiv:hep-ph/0601001](https://arxiv.org/abs/hep-ph/0601001) [hep-ph].
- [14] F. Feruglio, C. Hagedorn, Y. Lin, and L. Merlo, “Lepton Flavour Violation in Models with $A(4)$ Flavour Symmetry,” *Nucl. Phys.* **B809** (2009) 218–243, [arXiv:0807.3160](https://arxiv.org/abs/0807.3160) [hep-ph].
- [15] F. Feruglio, C. Hagedorn, Y. Lin, and L. Merlo, “Lepton Flavour Violation in a Supersymmetric Model with $A(4)$ Flavour Symmetry,” *Nucl. Phys.* **B832** (2010) 251–288, [arXiv:0911.3874](https://arxiv.org/abs/0911.3874) [hep-ph].
- [16] M.-C. Chen and S. F. King, “ A_4 See-Saw Models and Form Dominance,” *JHEP* **06** (2009) 072, [arXiv:0903.0125](https://arxiv.org/abs/0903.0125) [hep-ph].
- [17] I. de Medeiros Varzielas and L. Merlo, “Ultraviolet Completion of Flavour Models,” *JHEP* **02** (2011) 062, [arXiv:1011.6662](https://arxiv.org/abs/1011.6662) [hep-ph].
- [18] G. Altarelli, F. Feruglio, L. Merlo, and E. Stamou, “Discrete Flavour Groups, θ_{13} and Lepton Flavour Violation,” *JHEP* **08** (2012) 021, [arXiv:1205.4670](https://arxiv.org/abs/1205.4670) [hep-ph].
- [19] Y. H. Ahn and S. K. Kang, “Non-zero θ_{13} and CP violation in a model with A_4 flavor symmetry,” *Phys. Rev.* **D86** (2012) 093003, [arXiv:1203.4185](https://arxiv.org/abs/1203.4185) [hep-ph].
- [20] N. Memenga, W. Rodejohann, and H. Zhang, “ A_4 flavor symmetry model for Dirac neutrinos and sizable U_{e3} ,” *Phys. Rev.* **D87** no. 5, (2013) 053021, [arXiv:1301.2963](https://arxiv.org/abs/1301.2963) [hep-ph].
- [21] R. Gonzalez Felipe, H. Serodio, and J. P. Silva, “Neutrino masses and mixing in A_4 models with three Higgs doublets,” *Phys. Rev.* **D88** no. 1, (2013) 015015, [arXiv:1304.3468](https://arxiv.org/abs/1304.3468) [hep-ph].
- [22] I. de Medeiros Varzielas and D. Pridt, “UV completions of flavour models and large θ_{13} ,” *JHEP* **03** (2013) 065, [arXiv:1211.5370](https://arxiv.org/abs/1211.5370) [hep-ph].
- [23] H. Ishimori and E. Ma, “New Simple A_4 Neutrino Model for Nonzero θ_{13} and Large δ_{CP} ,” *Phys. Rev.* **D86** (2012) 045030, [arXiv:1205.0075](https://arxiv.org/abs/1205.0075) [hep-ph].
- [24] S. F. King, S. Morisi, E. Peinado, and J. W. F. Valle, “Quark-Lepton Mass Relation in a Realistic A_4 Extension of the Standard Model,” *Phys. Lett.* **B724** (2013) 68–72, [arXiv:1301.7065](https://arxiv.org/abs/1301.7065) [hep-ph].
- [25] A. E. Carcamo Hernandez, I. de Medeiros Varzielas, S. G. Kovalenko, H. Päs, and I. Schmidt, “Lepton masses and mixings in an A_4 multi-Higgs model with a radiative seesaw mechanism,” *Phys. Rev.* **D88** no. 7, (2013) 076014, [arXiv:1307.6499](https://arxiv.org/abs/1307.6499) [hep-ph].
- [26] K. S. Babu, E. Ma, and J. W. F. Valle, “Underlying $A(4)$ symmetry for the neutrino mass matrix and the quark mixing matrix,” *Phys. Lett.* **B552** (2003) 207–213, [arXiv:hep-ph/0206292](https://arxiv.org/abs/hep-ph/0206292) [hep-ph].
- [27] G. Altarelli and F. Feruglio, “Tri-bimaximal neutrino mixing, $A(4)$ and the modular symmetry,” *Nucl. Phys.* **B741** (2006) 215–235, [arXiv:hep-ph/0512103](https://arxiv.org/abs/hep-ph/0512103) [hep-ph].
- [28] S. Gupta, A. S. Joshipura, and K. M. Patel, “Minimal extension of tri-bimaximal mixing and generalized $Z_2 \rightarrow Z_2$ symmetries,” *Phys. Rev.* **D85** (2012) 031903, [arXiv:1112.6113](https://arxiv.org/abs/1112.6113) [hep-ph].
- [29] S. Morisi, M. Nebot, K. M. Patel, E. Peinado, and J. W. F. Valle, “Quark-Lepton Mass Relation and CKM mixing in an A_4 Extension of the Minimal Supersymmetric Standard Model,” *Phys. Rev.* **D88** (2013) 036001, [arXiv:1303.4394](https://arxiv.org/abs/1303.4394) [hep-ph].
- [30] G. Altarelli and F. Feruglio, “Tri-bimaximal neutrino mixing from discrete symmetry in extra dimensions,” *Nucl. Phys.* **B720** (2005) 64–88, [arXiv:hep-ph/0504165](https://arxiv.org/abs/hep-ph/0504165) [hep-ph].
- [31] A. Kadosh and E. Pallante, “An $A(4)$ flavor model for quarks and leptons in warped geometry,” *JHEP* **08** (2010) 115, [arXiv:1004.0321](https://arxiv.org/abs/1004.0321) [hep-ph].
- [32] A. Kadosh, “ Θ_{13} and charged Lepton Flavor Violation in “warped” A_4 models,” *JHEP* **06** (2013) 114, [arXiv:1303.2645](https://arxiv.org/abs/1303.2645) [hep-ph].
- [33] F. del Aguila, A. Carmona, and J. Santiago, “Neutrino Masses from an A_4 Symmetry in Holographic Composite Higgs Models,” *JHEP* **08** (2010) 127, [arXiv:1001.5151](https://arxiv.org/abs/1001.5151) [hep-ph].
- [34] M. D. Campos, A. E. Cárcamo Hernández, S. Kovalenko, I. Schmidt, and E. Schumacher, “Fermion masses and mixings in an $SU(5)$ grand unified model with an extra flavor symmetry,” *Phys. Rev.* **D90** no. 1, (2014) 016006, [arXiv:1403.2525](https://arxiv.org/abs/1403.2525) [hep-ph].
- [35] V. V. Vien and H. N. Long, “Neutrino mixing with nonzero θ_{13} and CP violation in the 3-3-1 model based on A_4 flavor symmetry,” *Int. J. Mod. Phys.* **A30** no. 21, (2015) 1550117, [arXiv:1405.4665](https://arxiv.org/abs/1405.4665) [hep-ph].
- [36] A. S. Joshipura and K. M. Patel, “Generalized μ - τ symmetry and discrete subgroups of $O(3)$,” *Phys. Lett.* **B749** (2015) 159–166, [arXiv:1507.01235](https://arxiv.org/abs/1507.01235) [hep-ph].
- [37] A. E. Cárcamo Hernández and R. Martínez, “A predictive 3-3-1 model with A_4 flavor symmetry,” *Nucl. Phys.* **B905** (2016) 337–358, [arXiv:1501.05937](https://arxiv.org/abs/1501.05937) [hep-ph].
- [38] B. Karmakar and A. Sil, “An A_4 realization of inverse seesaw: neutrino masses, θ_{13} and leptonic non-unitarity,” *Phys. Rev.* **D96** no. 1, (2017) 015007, [arXiv:1610.01909](https://arxiv.org/abs/1610.01909) [hep-ph].
- [39] D. Borah and B. Karmakar, “ A_4 flavour model for Dirac neutrinos: Type I and inverse seesaw,” *Phys. Lett.* **B780** (2018) 461–470, [arXiv:1712.06407](https://arxiv.org/abs/1712.06407) [hep-ph].

- [40] P. Chattopadhyay and K. M. Patel, “Discrete symmetries for electroweak natural type-I seesaw mechanism,” *Nucl. Phys.* **B921** (2017) 487–506, [arXiv:1703.09541 \[hep-ph\]](#).
- [41] A. E. Cárcamo Hernández and H. N. Long, “A highly predictive A_4 flavour 3-3-1 model with radiative inverse seesaw mechanism,” *J. Phys.* **G45** no. 4, (2018) 045001, [arXiv:1705.05246 \[hep-ph\]](#).
- [42] E. Ma and G. Rajasekaran, “Cobimaximal neutrino mixing from A_4 and its possible deviation,” *EPL* **119** no. 3, (2017) 31001, [arXiv:1708.02208 \[hep-ph\]](#).
- [43] S. Centelles Chuliá, R. Srivastava, and J. W. F. Valle, “Generalized Bottom-Tau unification, neutrino oscillations and dark matter: predictions from a lepton quarticity flavor approach,” *Phys. Lett.* **B773** (2017) 26–33, [arXiv:1706.00210 \[hep-ph\]](#).
- [44] F. Björkeröth, E. J. Chun, and S. F. King, “Accidental Peccei–Quinn symmetry from discrete flavour symmetry and Pati–Salam,” *Phys. Lett.* **B777** (2018) 428–434, [arXiv:1711.05741 \[hep-ph\]](#).
- [45] R. Srivastava, C. A. Ternes, M. Tórtola, and J. W. F. Valle, “Testing a lepton quarticity flavor theory of neutrino oscillations with the DUNE experiment,” *Phys. Lett.* **B778** (2018) 459–463, [arXiv:1711.10318 \[hep-ph\]](#).
- [46] A. S. Belyaev, S. F. King, and P. B. Schaefer, “Muon g-2 and dark matter suggest nonuniversal gaugino masses: $SU(5) \times A_4$ case study at the LHC,” *Phys. Rev.* **D97** no. 11, (2018) 115002, [arXiv:1801.00514 \[hep-ph\]](#).
- [47] A. E. Cárcamo Hernández and S. F. King, “Muon anomalies and the $SU(5)$ Yukawa relations,” *Phys. Rev.* **D99** no. 9, (2019) 095003, [arXiv:1803.07367 \[hep-ph\]](#).
- [48] R. Srivastava, C. A. Ternes, M. Tórtola, and J. W. F. Valle, “Zooming in on neutrino oscillations with DUNE,” *Phys. Rev.* **D97** no. 9, (2018) 095025, [arXiv:1803.10247 \[hep-ph\]](#).
- [49] L. M. G. De La Vega, R. Ferro-Hernandez, and E. Peinado, “Simple A_4 models for dark matter stability with texture zeros,” *Phys. Rev.* **D99** no. 5, (2019) 055044, [arXiv:1811.10619 \[hep-ph\]](#).
- [50] D. Borah and B. Karmakar, “Linear seesaw for Dirac neutrinos with A_4 flavour symmetry,” *Phys. Lett.* **B789** (2019) 59–70, [arXiv:1806.10685 \[hep-ph\]](#).
- [51] S. Pramanick, “Radiative generation of realistic neutrino mixing with A_4 ,” *Nucl. Phys.* **B963** (2021) 115282, [arXiv:1903.04208 \[hep-ph\]](#).
- [52] A. E. Cárcamo Hernández, J. Marchant González, and U. J. Saldaña-Salazar, “Viable low-scale model with universal and inverse seesaw mechanisms,” *Phys. Rev.* **D100** no. 3, (2019) 035024, [arXiv:1904.09993 \[hep-ph\]](#).
- [53] A. E. Cárcamo Hernández, M. González, and N. A. Neill, “Low scale type I seesaw model for lepton masses and mixings,” *Phys. Rev.* **D101** no. 3, (2020) 035005, [arXiv:1906.00978 \[hep-ph\]](#).
- [54] G.-J. Ding, S. F. King, and X.-G. Liu, “Modular A_4 symmetry models of neutrinos and charged leptons,” *JHEP* **09** (2019) 074, [arXiv:1907.11714 \[hep-ph\]](#).
- [55] H. Okada and M. Tanimoto, “Towards unification of quark and lepton flavors in A_4 modular invariance,” *Eur. Phys. J.* **C81** no. 1, (2021) 52, [arXiv:1905.13421 \[hep-ph\]](#).
- [56] F. Pisano and V. Pleitez, “An $SU(3) \times U(1)$ model for electroweak interactions,” *Phys. Rev. D* **46** (1992) 410–417, [arXiv:hep-ph/9206242](#).
- [57] P. H. Frampton, “Chiral dilepton model and the flavor question,” *Phys. Rev. Lett.* **69** (Nov, 1992) 2889–2891. <https://link.aps.org/doi/10.1103/PhysRevLett.69.2889>.
- [58] M. Singer, J. W. F. Valle, and J. Schechter, “Canonical neutral-current predictions from the weak-electromagnetic gauge group $su(3) \times u(1)$,” *Phys. Rev. D* **22** (Aug, 1980) 738–743. <https://link.aps.org/doi/10.1103/PhysRevD.22.738>.
- [59] J. C. Montero, F. Pisano, and V. Pleitez, “Neutral currents and GIM mechanism in $SU(3)$ -L \times $U(1)$ -N models for electroweak interactions,” *Phys. Rev. D* **47** (1993) 2918–2929, [arXiv:hep-ph/9212271](#).
- [60] A. Doff and F. Pisano, “Charge quantization in the largest leptoquark bilepton chiral electroweak scheme,” *Mod. Phys. Lett. A* **14** (1999) 1133–1142, [arXiv:hep-ph/9812303](#).
- [61] C. A. de Sousa Pires and O. P. Ravinez, “Charge quantization in a chiral bilepton gauge model,” *Phys. Rev. D* **58** (1998) 035008, [arXiv:hep-ph/9803409](#).
- [62] C. A. de Sousa Pires, “Remark on the vector - like nature of the electromagnetism and the electric charge quantization,” *Phys. Rev. D* **60** (1999) 075013, [arXiv:hep-ph/9902406](#).
- [63] P. V. Dong and H. N. Long, “Electric charge quantization in $SU(3)(C) \times SU(3)(L) \times U(1)(X)$ models,” *Int. J. Mod. Phys. A* **21** (2006) 6677–6692, [arXiv:hep-ph/0507155](#).
- [64] P. V. Dong, H. N. Long, and H. T. Hung, “Question of Peccei-Quinn symmetry and quark masses in the economical 3-3-1 model,” *Phys. Rev. D* **86** (2012) 033002, [arXiv:1205.5648 \[hep-ph\]](#).
- [65] P. B. Pal, “The Strong CP question in $SU(3)(C) \times SU(3)(L) \times U(1)(N)$ models,” *Phys. Rev. D* **52** (1995) 1659–1662, [arXiv:hep-ph/9411406](#).
- [66] A. G. Dias and V. Pleitez, “Stabilizing the invisible axion in 3-3-1 models,” *Phys. Rev. D* **69** (2004) 077702, [arXiv:hep-ph/0308037](#).
- [67] M. B. Tully and G. C. Joshi, “Generating neutrino mass in the 331 model,” *Phys. Rev.* **D64** (2001) 011301, [arXiv:hep-ph/0011172 \[hep-ph\]](#).
- [68] A. G. Dias, C. A. de S. Pires, and P. S. Rodrigues da Silva, “Naturally light right-handed neutrinos in a 3-3-1 model,” *Phys. Lett.* **B628** (2005) 85–92, [arXiv:hep-ph/0508186 \[hep-ph\]](#).
- [69] D. Chang and H. N. Long, “Interesting radiative patterns of neutrino mass in an $SU(3)(C) \times SU(3)(L) \times U(1)(X)$ model with right-handed neutrinos,” *Phys. Rev.* **D73** (2006) 053006, [arXiv:hep-ph/0603098 \[hep-ph\]](#).
- [70] P. V. Dong, H. N. Long, and D. V. Soa, “Neutrino masses in the economical 3-3-1 model,” *Phys. Rev.* **D75** (2007) 073006, [arXiv:hep-ph/0610381 \[hep-ph\]](#).
- [71] P. V. Dong and H. N. Long, “Neutrino masses and lepton flavor violation in the 3-3-1 model with right-handed

- neutrinos,” *Phys. Rev.* **D77** (2008) 057302, [arXiv:0801.4196 \[hep-ph\]](#).
- [72] P. V. Dong, L. T. Hue, H. N. Long, and D. V. Soa, “The 3-3-1 model with A_4 flavor symmetry,” *Phys. Rev.* **D81** (2010) 053004, [arXiv:1001.4625 \[hep-ph\]](#).
- [73] P. V. Dong, H. N. Long, D. V. Soa, and V. V. Vien, “The 3-3-1 model with S_4 flavor symmetry,” *Eur. Phys. J.* **C71** (2011) 1544, [arXiv:1009.2328 \[hep-ph\]](#).
- [74] P. V. Dong, H. N. Long, C. H. Nam, and V. V. Vien, “The S_3 flavor symmetry in 3-3-1 models,” *Phys. Rev.* **D85** (2012) 053001, [arXiv:1111.6360 \[hep-ph\]](#).
- [75] S. M. Boucenna, S. Morisi, and J. W. F. Valle, “Radiative neutrino mass in 3-3-1 scheme,” *Phys. Rev.* **D90** no. 1, (2014) 013005, [arXiv:1405.2332 \[hep-ph\]](#).
- [76] S. M. Boucenna, R. M. Fonseca, F. Gonzalez-Canales, and J. W. F. Valle, “Small neutrino masses and gauge coupling unification,” *Phys. Rev.* **D91** no. 3, (2015) 031702, [arXiv:1411.0566 \[hep-ph\]](#).
- [77] S. M. Boucenna, J. W. F. Valle, and A. Vicente, “Predicting charged lepton flavor violation from 3-3-1 gauge symmetry,” *Phys. Rev.* **D92** no. 5, (2015) 053001, [arXiv:1502.07546 \[hep-ph\]](#).
- [78] H. Okada, N. Okada, and Y. Orikasa, “Radiative seesaw mechanism in a minimal 3-3-1 model,” *Phys. Rev.* **D93** no. 7, (2016) 073006, [arXiv:1504.01204 \[hep-ph\]](#).
- [79] C. A. de S. Pires, “Neutrino mass mechanisms in 3-3-1 models: A short review,” *Physics International* **6** (Aug, 2015) 33–41, [arXiv:1412.1002 \[hep-ph\]](#). <https://thescpub.com/abstract/pisp.2015.33.41>.
- [80] A. G. Dias, C. A. de S. Pires, and P. S. Rodrigues da Silva, “The Left-Right $SU(3)(L) \times SU(3)(R) \times U(1)(X)$ Model with Light, keV and Heavy Neutrinos,” *Phys. Rev.* **D82** (2010) 035013, [arXiv:1003.3260 \[hep-ph\]](#).
- [81] D. T. Huong and P. V. Dong, “Left-right asymmetry and 750 GeV diphoton excess,” *Phys. Rev.* **D93** no. 9, (2016) 095019, [arXiv:1603.05146 \[hep-ph\]](#).
- [82] M. Reig, J. W. F. Valle, and C. A. Vaquera-Araujo, “Unifying left-right symmetry and 331 electroweak theories,” *Phys. Lett.* **B766** (2017) 35–40, [arXiv:1611.02066 \[hep-ph\]](#).
- [83] F. Pisano, D. Gomez Dumm, F. Pisano, and V. Pleitez, “Flavor changing neutral currents in $SU(3) \times U(1)$ models,” *Mod. Phys. Lett.* **A9** (1994) 1609–1615, [arXiv:hep-ph/9307265 \[hep-ph\]](#).
- [84] A. J. Buras, F. De Fazio, J. Girrbach, and M. V. Carlucci, “The Anatomy of Quark Flavour Observables in 331 Models in the Flavour Precision Era,” *JHEP* **02** (2013) 023, [arXiv:1211.1237 \[hep-ph\]](#).
- [85] A. J. Buras, F. De Fazio, and J. Girrbach, “331 models facing new $b \rightarrow s\mu^+\mu^-$ data,” *JHEP* **02** (2014) 112, [arXiv:1311.6729 \[hep-ph\]](#).
- [86] R. Gauld, F. Goertz, and U. Haisch, “An explicit Z' -boson explanation of the $B \rightarrow K^*\mu^+\mu^-$ anomaly,” *JHEP* **01** (2014) 069, [arXiv:1310.1082 \[hep-ph\]](#).
- [87] A. J. Buras, F. De Fazio, and J. Girrbach-Noe, “ Z - Z' mixing and Z -mediated FCNCs in $SU(3)_C \times SU(3)_L \times U(1)_X$ models,” *JHEP* **08** (2014) 039, [arXiv:1405.3850 \[hep-ph\]](#).
- [88] A. J. Buras and F. De Fazio, “ ϵ'/ϵ in 331 Models,” *JHEP* **03** (2016) 010, [arXiv:1512.02869 \[hep-ph\]](#).
- [89] P. Van Dong, N. T. K. Ngan, T. Tham, L. Thien, and N. Thuy, “Phenomenology of the simple 3-3-1 model with inert scalars,” *Phys. Rev.* **D99** no. 9, (2019) 095031, [arXiv:1512.09073 \[hep-ph\]](#).
- [90] V. H. Binh, C. Bonilla, A. E. Cárcamo Hernández, D. T. Huong, V. K. N., H. N. Long, P. N. Thu, and I. Schmidt, “Phenomenology of 3-3-1 models with a radiative inverse seesaw mechanism,” *Phys. Rev. D* **110** no. 7, (2024) 075022, [arXiv:2404.13373 \[hep-ph\]](#).
- [91] P. N. Thu, N. T. Duy, A. E. Carcamo Hernandez, and D. T. Huong, “Lepton universality violation in the minimal flipped 331 model,” *PTEP* **2023** no. 12, (2023) 123B01, [arXiv:2304.03003 \[hep-ph\]](#).
- [92] N. T. Duy, P. N. Thu, and D. T. Huong, “New physics in $b \rightarrow s$ transitions in the MF331 model,” *Eur. Phys. J. C* **82** no. 10, (2022) 966, [arXiv:2205.02995 \[hep-ph\]](#).
- [93] D. Nguyen Tuan, T. Inami, and H. Do Thi, “Physical constraints derived from FCNC in the 3-3-1-1 model,” *Eur. Phys. J. C* **81** no. 9, (2021) 813, [arXiv:2009.09698 \[hep-ph\]](#).
- [94] D. T. Huong and N. T. Duy, “Investigation of the Higgs boson anomalous FCNC interactions in the simple 3-3-1 model,” *Eur. Phys. J. C* **80** no. 5, (2020) 439, [arXiv:2002.01115 \[hep-ph\]](#).
- [95] D. Fregolente and M. D. Tonasse, “Selfinteracting dark matter from an $SU(3)(L) \times U(1)(N)$ electroweak model,” *Phys. Lett.* **B555** (2003) 7–12, [arXiv:hep-ph/0209119 \[hep-ph\]](#).
- [96] H. N. Long and N. Q. Lan, “Selfinteracting dark matter and Higgs bosons in the $SU(3)(C) \times SU(3)(L) \times U(1)(N)$ model with right-handed neutrinos,” *Europhys. Lett.* **64** (2003) 571, [arXiv:hep-ph/0309038 \[hep-ph\]](#).
- [97] S. Filippi, W. A. Ponce, and L. A. Sanchez, “Dark matter from the scalar sector of 3-3-1 models without exotic electric charges,” *Europhys. Lett.* **73** (2006) 142–148, [arXiv:hep-ph/0509173 \[hep-ph\]](#).
- [98] C. A. de S. Pires and P. S. Rodrigues da Silva, “Scalar Bilepton Dark Matter,” *JCAP* **0712** (2007) 012, [arXiv:0710.2104 \[hep-ph\]](#).
- [99] J. K. Mizukoshi, C. A. de S. Pires, F. S. Queiroz, and P. S. Rodrigues da Silva, “WIMPs in a 3-3-1 model with heavy Sterile neutrinos,” *Phys. Rev.* **D83** (2011) 065024, [arXiv:1010.4097 \[hep-ph\]](#).
- [100] J. D. Ruiz-Alvarez, C. A. de S. Pires, F. S. Queiroz, D. Restrepo, and P. S. Rodrigues da Silva, “On the Connection of Gamma-Rays, Dark Matter and Higgs Searches at LHC,” *Phys. Rev.* **D86** (2012) 075011, [arXiv:1206.5779 \[hep-ph\]](#).
- [101] S. Profumo and F. S. Queiroz, “Constraining the Z' mass in 331 models using direct dark matter detection,” *Eur. Phys. J. C* **74** no. 7, (2014) 2960, [arXiv:1307.7802 \[hep-ph\]](#).
- [102] C. Kelso, C. A. de S. Pires, S. Profumo, F. S. Queiroz, and P. S. Rodrigues da Silva, “A 331 WIMP Dark Radiation Model,” *Eur. Phys. J. C* **74** no. 3, (2014) 2797, [arXiv:1308.6630 \[hep-ph\]](#).
- [103] P. S. Rodrigues da Silva, “A Brief Review on WIMPs in 331 Electroweak Gauge Models,” *Phys. Int.* **7** no. 1, (2016)

- 15–27, [arXiv:1412.8633 \[hep-ph\]](#).
- [104] P. V. Dong, T. P. Nguyen, and D. V. Soa, “3-3-1 model with inert scalar triplet,” *Phys. Rev.* **D88** no. 9, (2013) 095014, [arXiv:1308.4097 \[hep-ph\]](#).
- [105] P. V. Dong, N. T. K. Ngan, and D. V. Soa, “Simple 3-3-1 model and implication for dark matter,” *Phys. Rev.* **D90** no. 7, (2014) 075019, [arXiv:1407.3839 \[hep-ph\]](#).
- [106] P. V. Dong, C. S. Kim, D. V. Soa, and N. T. Thuy, “Investigation of Dark Matter in Minimal 3-3-1 Models,” *Phys. Rev.* **D91** no. 11, (2015) 115019, [arXiv:1501.04385 \[hep-ph\]](#).
- [107] P. V. Dong, H. T. Hung, and T. D. Tham, “3-3-1-1 model for dark matter,” *Phys. Rev.* **D87** no. 11, (2013) 115003, [arXiv:1305.0369 \[hep-ph\]](#).
- [108] P. V. Dong, D. T. Huong, F. S. Queiroz, and N. T. Thuy, “Phenomenology of the 3-3-1-1 model,” *Phys. Rev.* **D90** no. 7, (2014) 075021, [arXiv:1405.2591 \[hep-ph\]](#).
- [109] P. V. Dong, “Unifying the electroweak and B-L interactions,” *Phys. Rev.* **D92** no. 5, (2015) 055026, [arXiv:1505.06469 \[hep-ph\]](#).
- [110] D. T. Huong and P. V. Dong, “Neutrino masses and superheavy dark matter in the 3-3-1-1 model,” *Eur. Phys. J.* **C77** no. 4, (2017) 204, [arXiv:1605.01216 \[hep-ph\]](#).
- [111] A. Alves, G. Arcadi, P. V. Dong, L. Duarte, F. S. Queiroz, and J. W. F. Valle, “Matter-parity as a residual gauge symmetry: Probing a theory of cosmological dark matter,” *Phys. Lett.* **B772** (2017) 825–831, [arXiv:1612.04383 \[hep-ph\]](#).
- [112] C. P. Ferreira, M. M. Guzzo, and P. C. de Holanda, “Cosmological bounds of sterile neutrinos in a $SU(3)_C \otimes SU(3)_L \otimes SU(3)_R \otimes U(1)_N$ model as dark matter candidates,” *Braz. J. Phys.* **46** no. 4, (2016) 453–461, [arXiv:1509.02977 \[hep-ph\]](#).
- [113] P. V. Dong, D. T. Huong, F. S. Queiroz, J. W. F. Valle, and C. A. Vaquera-Araujo, “The Dark Side of Flipped Trification,” *JHEP* **04** (2018) 143, [arXiv:1710.06951 \[hep-ph\]](#).
- [114] D. T. Huong, P. V. Dong, C. S. Kim, and N. T. Thuy, “Inflation and leptogenesis in the 3-3-1-1 model,” *Phys. Rev.* **D91** (2015) 055023, [arXiv:1501.00543 \[hep-ph\]](#).
- [115] P. Van Dong, D. T. Huong, D. A. Camargo, F. S. Queiroz, and J. W. F. Valle, “Asymmetric Dark Matter, Inflation and Leptogenesis from $B - L$ Symmetry Breaking,” *Phys. Rev.* **D99** no. 5, (2019) 055040, [arXiv:1805.08251 \[hep-ph\]](#).
- [116] P. V. Dong, D. Q. Phong, D. V. Soa, and N. C. Thao, “The economical 3-3-1 model revisited,” *Eur. Phys. J. C* **78** no. 8, (2018) 653, [arXiv:1706.06152 \[hep-ph\]](#).
- [117] Y. Shimizu, M. Tanimoto, and A. Watanabe, “Breaking Tri-bimaximal Mixing and Large θ_{13} ,” *Prog. Theor. Phys.* **126** (2011) 81–90, [arXiv:1105.2929 \[hep-ph\]](#).
- [118] T. Kobayashi, N. Omoto, Y. Shimizu, K. Takagi, M. Tanimoto, and T. H. Tatsuishi, “Modular A_4 invariance and neutrino mixing,” *JHEP* **11** (2018) 196, [arXiv:1808.03012 \[hep-ph\]](#).
- [119] A. E. Cárcamo Hernández, S. Kovalenko, H. N. Long, and I. Schmidt, “A variant of 3-3-1 model for the generation of the SM fermion mass and mixing pattern,” *JHEP* **07** (2018) 144, [arXiv:1705.09169 \[hep-ph\]](#).
- [120] A. E. Cárcamo Hernández, D. T. Huong, and H. N. Long, “Minimal model for the fermion flavor structure, mass hierarchy, dark matter, leptogenesis, and the electron and muon anomalous magnetic moments,” *Phys. Rev. D* **102** no. 5, (2020) 055002, [arXiv:1910.12877 \[hep-ph\]](#).
- [121] A. Cárcamo Hernández, J. Marchant González, D. Salinas-Arizmendi, and M. Mora-Urrutia, “Phenomenological aspects of the fermion and scalar sectors of a s_4 flavored 3-3-1 model,” *Nuclear Physics B* **1005** (2024) 116588. <https://www.sciencedirect.com/science/article/pii/S0550321324001548>.
- [122] K. Bora, “Updated values of running quark and lepton masses at GUT scale in SM, 2HDM and MSSM,” *Horizon* **2** (2013) 112, [arXiv:1206.5909 \[hep-ph\]](#).
- [123] Z.-z. Xing, H. Zhang, and S. Zhou, “Updated Values of Running Quark and Lepton Masses,” *Phys. Rev.* **D77** (2008) 113016, [arXiv:0712.1419 \[hep-ph\]](#).
- [124] **Particle Data Group** Collaboration, M. Tanabashi *et al.*, “Review of Particle Physics,” *Phys. Rev.* **D98** no. 3, (2018) 030001.
- [125] Q.-H. Cao and D.-M. Zhang, “Collider Phenomenology of the 3-3-1 Model,” [arXiv:1611.09337 \[hep-ph\]](#).
- [126] J. A. Aguilar-Saavedra, F. Deppisch, O. Kittel, and J. W. F. Valle, “Flavour in heavy neutrino searches at the LHC,” *Phys. Rev.* **D85** (2012) 091301, [arXiv:1203.5998 \[hep-ph\]](#).
- [127] S. P. Das, F. F. Deppisch, O. Kittel, and J. W. F. Valle, “Heavy Neutrinos and Lepton Flavour Violation in Left-Right Symmetric Models at the LHC,” *Phys. Rev.* **D86** (2012) 055006, [arXiv:1206.0256 \[hep-ph\]](#).
- [128] A. Das and N. Okada, “Inverse seesaw neutrino signatures at the LHC and ILC,” *Phys. Rev. D* **88** (2013) 113001, [arXiv:1207.3734 \[hep-ph\]](#).
- [129] P. S. Bhupal Dev, R. Franceschini, and R. N. Mohapatra, “Bounds on TeV Seesaw Models from LHC Higgs Data,” *Phys. Rev. D* **86** (2012) 093010, [arXiv:1207.2756 \[hep-ph\]](#).
- [130] J. C. Helo, H. Li, N. A. Neill, M. Ramsey-Musolf, and J. C. Vasquez, “Probing neutrino Dirac mass in left-right symmetric models at the LHC and next generation colliders,” *Phys. Rev. D* **99** no. 5, (2019) 055042, [arXiv:1812.01630 \[hep-ph\]](#).
- [131] S. Pascoli, R. Ruiz, and C. Weiland, “Heavy neutrinos with dynamic jet vetoes: multilepton searches at $\sqrt{s} = 14, 27,$ and 100 TeV,” *JHEP* **06** (2019) 049, [arXiv:1812.08750 \[hep-ph\]](#).
- [132] I. Esteban, M. C. Gonzalez-Garcia, M. Maltoni, T. Schwetz, and A. Zhou, “The fate of hints: updated global analysis of three-flavor neutrino oscillations,” *JHEP* **09** (2020) 178, [arXiv:2007.14792 \[hep-ph\]](#).
- [133] **KamLAND-Zen** Collaboration, S. Abe *et al.*, “Search for the Majorana Nature of Neutrinos in the Inverted Mass

- Ordering Region with KamLAND-Zen,” *Phys. Rev. Lett.* **130** no. 5, (2023) 051801, [arXiv:2203.02139 \[hep-ex\]](#).
- [134] A. E. C. Hernández, L. Duarte, A. S. de Jesus, S. Kovalenko, F. S. Queiroz, C. Siqueira, Y. M. Oviedo-Torres, and Y. Villamizar, “Flavor changing interactions confronted with meson mixing and hadron colliders,” *Phys. Rev. D* **107** (Mar, 2023) 063005. <https://link.aps.org/doi/10.1103/PhysRevD.107.063005>.
- [135] T. T. Hong, L. T. Hue, L. T. T. Phuong, N. H. T. Nha, and T. P. Nguyen, “Decays $Z \rightarrow e_a e_b$ in a 3-3-1 model with neutral leptons,” *Phys. Scripta* **99** no. 12, (2024) 125308, [arXiv:2406.11040 \[hep-ph\]](#).
- [136] LHCb Collaboration, R. Aaij *et al.*, “Search for the lepton-flavour violating decay $D^0 \rightarrow e^\pm \mu^\mp$,” *Phys. Lett. B* **754** (2016) 167–175, [arXiv:1512.00322 \[hep-ex\]](#).
- [137] P. C. Awasthi, J. More, A. K. Pradhan, K. Rao, P. Sahu, and S. U. Sankar, “Charged Lepton Flavour Violating Meson Decays in Seesaw Models,” [arXiv:2410.10490 \[hep-ph\]](#).
- [138] Z. Gagyi-Palfy, A. Pilaftsis, and K. Schilcher, “Heavy neutrino chirality enhancement of the decay $K_L \rightarrow e\mu$ in left-right symmetric models,” *Phys. Lett. B* **343** (1995) 275–281, [arXiv:hep-ph/9410201](#).
- [139] M. E. Catano, R. Martinez, and F. Ochoa, “Neutrino masses in a 331 model with right-handed neutrinos without doubly charged Higgs bosons via inverse and double seesaw mechanisms,” *Phys. Rev. D* **86** (2012) 073015, [arXiv:1206.1966 \[hep-ph\]](#).
- [140] L. T. Hue, L. D. Ninh, T. T. Thuc, and N. T. T. Dat, “Exact one-loop results for $l_i \rightarrow l_j \gamma$ in 3-3-1 models,” *Eur. Phys. J. C* **78** no. 2, (2018) 128, [arXiv:1708.09723 \[hep-ph\]](#).
- [141] T. P. Nguyen, T. T. Le, T. T. Hong, and L. T. Hue, “Decay of standard model-like Higgs boson $h \rightarrow \mu\tau$ in a 3-3-1 model with inverse seesaw neutrino masses,” *Phys. Rev. D* **97** no. 7, (2018) 073003, [arXiv:1802.00429 \[hep-ph\]](#).
- [142] MEG II Collaboration, K. Afanaciev *et al.*, “A search for $\mu^+ \rightarrow e^+ \gamma$ with the first dataset of the MEG II experiment,” *Eur. Phys. J. C* **84** no. 3, (2024) 216, [arXiv:2310.12614 \[hep-ex\]](#). [Erratum: *Eur.Phys.J.C* 84, 1042 (2024)].
- [143] R. H. Bernstein and P. S. Cooper, “Charged Lepton Flavor Violation: An Experimenter’s Guide,” *Phys. Rept.* **532** (2013) 27–64, [arXiv:1307.5787 \[hep-ex\]](#).
- [144] E. Ma and M. Raidal, “Neutrino mass, muon anomalous magnetic moment, and lepton flavor nonconservation,” *Phys. Rev. Lett.* **87** (2001) 011802, [arXiv:hep-ph/0102255](#). [Erratum: *Phys.Rev.Lett.* 87, 159901 (2001)].
- [145] T. Toma and A. Vicente, “Lepton Flavor Violation in the Scotogenic Model,” *JHEP* **01** (2014) 160, [arXiv:1312.2840 \[hep-ph\]](#).
- [146] A. Vicente and C. E. Yaguna, “Probing the scotogenic model with lepton flavor violating processes,” *JHEP* **02** (2015) 144, [arXiv:1412.2545 \[hep-ph\]](#).
- [147] M. Lindner, M. Platscher, and F. S. Queiroz, “A Call for New Physics : The Muon Anomalous Magnetic Moment and Lepton Flavor Violation,” *Phys. Rept.* **731** (2018) 1–82, [arXiv:1610.06587 \[hep-ph\]](#).
- [148] A. E. Cárcamo Hernández, D. Salinas-Arizmendi, J. Vignatti, and A. Zerwekh, “Phenomenology of an Extended 1 + 2 Higgs Doublet Model with S_3 Family Symmetry,” *Eur. Phys. J. C* **84** (2024) 1135, [arXiv:2408.01497 \[hep-ph\]](#).
- [149] P. Wintz, “Results of the SINDRUM-II experiment,” *Conf. Proc. C* **980420** (1998) 534–546.
- [150] A. E. C. Hernández, H. N. Long, M. L. Mora-Urrutia, N. H. Thao, and V. V. Vien, “Fermion masses and mixings and $g - 2$ muon anomaly in a 3-3-1 model with D_4 family symmetry,” *Eur. Phys. J. C* **82** no. 8, (2022) 769, [arXiv:2104.04559 \[hep-ph\]](#).
- [151] Fermilab Lattice, LATTICE-HPQCD, MILC Collaboration, C. T. H. Davies *et al.*, “Hadronic-vacuum-polarization contribution to the muon’s anomalous magnetic moment from four-flavor lattice QCD,” *Phys. Rev. D* **101** no. 3, (2020) 034512, [arXiv:1902.04223 \[hep-lat\]](#).
- [152] S. Borsanyi *et al.*, “Leading hadronic contribution to the muon magnetic moment from lattice QCD,” *Nature* **593** no. 7857, (2021) 51–55, [arXiv:2002.12347 \[hep-lat\]](#).
- [153] C. Lehner and A. S. Meyer, “Consistency of hadronic vacuum polarization between lattice QCD and the R-ratio,” *Phys. Rev. D* **101** (2020) 074515, [arXiv:2003.04177 \[hep-lat\]](#).
- [154] C. Aubin, T. Blum, C. Tu, M. Golterman, C. Jung, and S. Peris, “Light quark vacuum polarization at the physical point and contribution to the muon $g - 2$,” *Phys. Rev. D* **101** no. 1, (2020) 014503, [arXiv:1905.09307 \[hep-lat\]](#).
- [155] H. Wittig, “Progress on $(g - 2)_\mu$ from Lattice QCD,” in *57th Rencontres de Moriond on Electroweak Interactions and Unified Theories*. 6, 2023. [arXiv:2306.04165 \[hep-ph\]](#).
- [156] D. Djukanovic, G. von Hippel, S. Kuberski, H. B. Meyer, N. Miller, K. Ottnad, J. Parrino, A. Risch, and H. Wittig, “The hadronic vacuum polarization contribution to the muon $g - 2$ at long distances,” [arXiv:2411.07969 \[hep-lat\]](#).
- [157] A. Crivellin, M. Hoferichter, and P. Schmidt-Wellenburg, “Combined explanations of $(g - 2)_{\mu,e}$ and implications for a large muon EDM,” *Phys. Rev. D* **98** no. 11, (2018) 113002, [arXiv:1807.11484 \[hep-ph\]](#).
- [158] F. F. Deppisch, N. Desai, and J. W. F. Valle, “Is charged lepton flavor violation a high energy phenomenon?,” *Phys. Rev. D* **89** no. 5, (2014) 051302, [arXiv:1308.6789 \[hep-ph\]](#).
- [159] H. Ishimori, T. Kobayashi, H. Ohki, Y. Shimizu, H. Okada, and M. Tanimoto, “Non-Abelian Discrete Symmetries in Particle Physics,” *Prog. Theor. Phys. Suppl.* **183** (2010) 1–163, [arXiv:1003.3552 \[hep-th\]](#).
- [160] G. Altarelli and F. Feruglio, “Discrete Flavor Symmetries and Models of Neutrino Mixing,” *Rev. Mod. Phys.* **82** (2010) 2701–2729, [arXiv:1002.0211 \[hep-ph\]](#).
- [161] S. F. King and C. Luhn, “Neutrino Mass and Mixing with Discrete Symmetry,” *Rept. Prog. Phys.* **76** (2013) 056201, [arXiv:1301.1340 \[hep-ph\]](#).
- [162] S. F. King, A. Merle, S. Morisi, Y. Shimizu, and M. Tanimoto, “Neutrino Mass and Mixing: from Theory to Experiment,” *New J. Phys.* **16** (2014) 045018, [arXiv:1402.4271 \[hep-ph\]](#).